The Impact of Bike Fitting on Biomechanical and Physiological Measures Between Sexes

MATTHEW PEARSON, University of Bath, United Kingdom

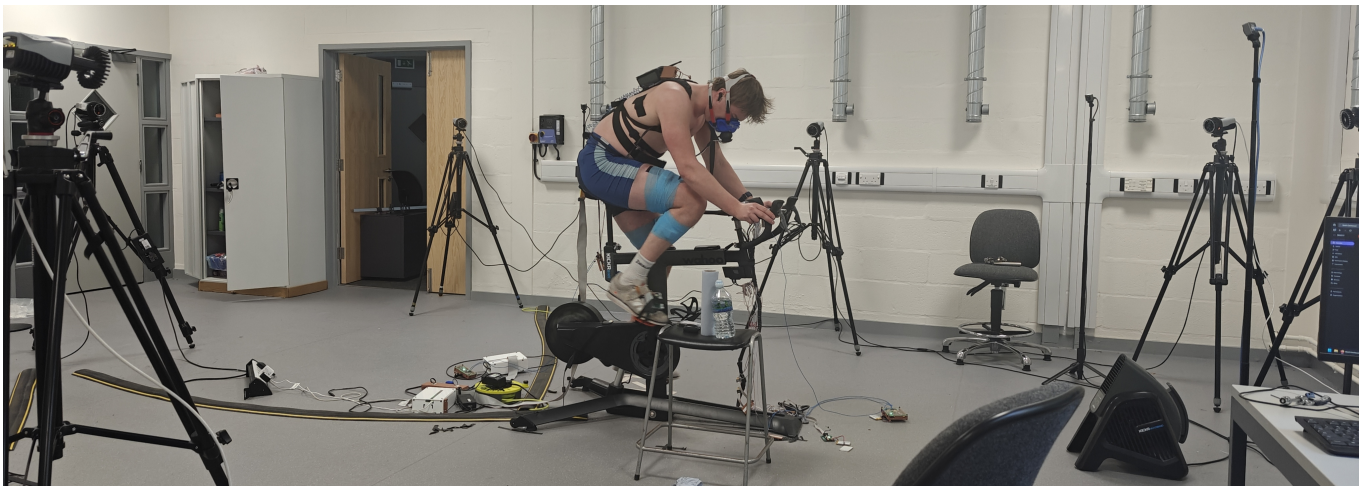


Fig. 1. Experimental setup showing a participant with sensors applied and on the static bike

Abstract: Bike fitting equations have historically been calibrated on male cohorts, yet anatomical interfaces (saddle, handlebars and cranks) differ between sexes due to variance in limb proportions and pelvic geometry. We collected multi-modal data (sEMG, NIRS, gas exchange, seatpost/handlebar strain, insole/saddle/handlebar pressure, IMU and markerless motion capture) from 51 cyclists (24 female, 27 male) before and after a standardised IBFI level-4 gross-road positioning fit (36 cyclists for paired analysis). A feature-level fusion pipeline compensated for measured metabolic lag. Two variables remained after FDR correction: VCO_2 and left-calf sEMG. Predicted sex-specific changes in saddle pressure and gluteal activation were not observed; instead, end-trial RPE fell by 0.6 in males but rose by 0.5 in females. Results support sex-specific fitting protocols and equipment over scaled male defaults.

Additional Key Words and Phrases: Multi-modal analysis, Interactive effects, sex-differences, Bike fitting, Cycling

1 Introduction

Non-traumatic overuse injuries affect up to 85% of cyclists, with poor bicycle fit identified as the primary cause (Dettori and Norvell, 2006). The standard solution is a bike fit, where adjustments redistribute load across contact points, allowing for sustained threshold work without sacrificing comfort (Burt, 2022). However, whether a fit produces measurable physiological improvements, how it produces those improvements, and for whom are questions that remain open. Industry practice relies on equational rules and user feedback rather than concurrent biomechanical and physiological measurement (Husband et al., 2024), and studies which have evaluated fit outcomes have done so one modality at a time (Millour et al., 2023). The problem this study seeks to address is that fitting is recommended for both injury prevention and performance gain there is no evidence base capable of determining what a successful fit changes within the rider, in which rider, or by which mechanism.

Published evidence on fit outcomes is partial; each modality has been studied in isolation but rarely concurrently. Professional fitting raises the probability of comfort improvement by a factor of 2.28 without significant effect on injury rates (Priego Quesada et al., 2019), and perceived comfort responds more sensitively to saddle-height adjustment than perceived exertion (Bini, 2020), suggesting that subjective measures track interface load before they track effort. Kinematic surveys document that fits change knee angles, postural drag and gross efficiency (Hoffmann et al., 2024; Fintelman et al., 2015). Chapman et al. (2009), however, showed that elite and novice cyclists with near-identical lower-limb kinematics had substantially different muscle recruitment patterns, meaning a rider seen as well-fitted on joint angles can be poorly-fitted on neuromuscular cost. Millour et al. (2023) extend this argument and claim that the metabolic penalty of a position cannot be inferred from kinematics alone, but requires concurrent neuromuscular and metabolic measurement. The studies that have attempted this remain small, methodologically heterogeneous and rarely sex-stratified (Husband et al., 2024). The field can therefore say that a fit moves comfort, kinematics and metabolic load, but cannot yet say which of these signals carries the fit response, nor whether equivalent inputs produce equivalent outputs across rider populations.

The population in which these gaps are most significant is female cyclists. Saddle-height formulae including LeMond and Guimard, Ferrer-Roca and the static goniometry framework were derived from almost exclusively male cohorts (Encarnación-Martínez et al., 2021), and a 2024 systematic review found that only 12.4% of participants in cycling biomechanics research were female (Husband et al., 2024). The same skew extends into industry; our IBFI level-4

Author's Contact Information: Matthew Pearson, University of Bath, Bath, United Kingdom, mp2457@bath.ac.uk.

fitter estimated that roughly 75% of his clients are males aged 40-65. Encarnación-Martínez et al. (2021) tested popular fitting equations and found that they predicted optimal knee angles for 47-60% of males but only 20-33% of females. Anatomy explains part of this gap: females present a wider ischial tuberosity and broader pubic arch ($> 90°$ vs. $< 90°$) (de Vey Mestdagh, 1998; Potter et al., 2008), a shorter arm-to-leg ratio (1.49 vs. 1.52) (Carpes et al., 2010) and a longer femur for a given leg length (Lin et al., 2023). The same forward pelvic tilt that unloads male ischial tuberosities concentrates load on the female pubic symphysis, raising soft-tissue injury risk (Larsen et al., 2018; Baran et al., 2014). The implication is that a single protocol applied to all riders may impose different physiological penalties, and that closing the evidence gap requires measurement that is sex-stratified for both equipment and protocol.

Commercial practice has so far moved against this evidence. In 2019 Specialized, Trek and Canyon stopped production of female-specific frames based on the claim that within-sex variability is as large as between-sex variability, leaving Liv as the only major manufacturer of female-specific frames (Torres-Davis, 2026). Testing the argument for sex-specific protocol requires multi-modal, sex-stratified data, which is lacking in the literature body potentially as manufacturers best placed to fund this research have exited the female-specific market. These following research gaps therefore reinforce each other: an absense of a mechanic account of fit removes industry's grounds to differentiate by sex, and the lack of sex-specific equipment leaves fitters applying male-derived equations to a population they were not calibrated against. (Encarnación-Martínez et al., 2021; Dixon et al., 2017). A controlled laboratory comparison of a standardised fit on both sexes, instrumented across different modalities, is the minimum needed to break this loop.

This study addresses three of the gaps identified above. We collected synchronised sEMG, NIRS, breath-by-breath gas exchange, IMU acceleration, saddle/handlebar/insole pressure, seatpost/handlebar strain, perceived effort and markerless motion-capture data from 51 cyclists (27 male, 24 female) before and after a standardised IBFI level-4 fit. The study evaluates a gross-road positioning fit, where protocol excluded aerodynamic optimisation and bar-width/saddle substitution, and aimed to minimise weight transmitted through the hands without sacrificing pedalling power or comfort (T. Corke, personal communication, 2026). A feature-level fusion pipeline synchronises the differing sample rates and physiological lags across modalities, allowing concurrent statistical analysis on a unified feature matrix. Sex-stratified comparisons test whether a single protocol produces equivalent responses between sexes, and supervised feature-importance analysis identifies which sensor modalities carry the most information about the fit.

Four research questions follow from the above gap analysis:
RQ1: Does a standardised professional bike fit produce significant pre-to-post changes in kinematic, neuromuscular, metabolic and pressure-distribution outcomes during threshold intensity cycling?
RQ2: Is there significant condition (pre- or post-fit) × sex interaction on these measures?
RQ3: Do neuromuscular features carry higher importance than kinematic features, and does this differ by sex?
RQ4: To what extent do changes across neuromuscular, kinematic and metabolic measures correlate, and do these correlations differ between sexes?

2 Related Work

2.1 Biomechanics in Bike Fitting

Bike fitting involves adjustments of spatial relationship between the rider and bicycle to find a balance of comfort, performance, and injury prevention. Burt (2022) argues that the idea of a single optimal position is flawed, as fit is influenced by variables including riding discipline, injury history, rider morphology, and will evolve over time. Competitive cycling requires optimisation of the trade-off between biomechanical power and drag forces, of which air resistance constitutes around 70% (Malizia and Blocken, 2021; Bouillod et al., 2016). Minimising frontal area through an "aggressive" riding position is therefore critical for increasing speed, but can compromise biomechanical efficiency and comfort (Malizia and Blocken, 2021). This balance is critical as non-traumatic overuse injuries affect up to 85% of cyclists, with poor fit identified as the primary cause (Dettori and Norvell, 2006).

Priego Quesada et al. (2019) found that professional bike fitting increases the probability of comfort improvement by a factor of 2.28, without significant effect on injury rates. Bini (2020) demonstrated that perceived comfort changes more sensitively compared to Rating of Perceived Exertion (RPE) in response to saddle height adjustment. This suggests that an assessment of fitting quality requires multiple measures that span biomechanical, physiological and subjective domains.

However, the literature surrounding fitting practice is constrained by multiple limitations. Husband et al. (2024) conducted a systematic review of biomechanical cycling studies and found that fit variables are typically investigated in isolation, neglecting interactive effects where a change in one aspect may alter a different one. Furthermore, fitting guidelines have been derived from populations that are not representative, with only 12.4% of participants in cycling biomechanics research being female. This under-representation also extends into the professional practice, with the fitter for this study confirming that approximately 75% of clients for fittings are 40-65 year-old males (Corke, 2026). This has led predictive models embedded in fitting practice to be calibrated on anatomies for which they were not intended to generalise from (Husband et al., 2024; Encarnación-Martínez et al., 2021).

2.2 Failures of Fitting Formulae

Widely used saddle height formulae such as LeMond and Guimard were derived from males with a mean height of approximately 1.78 m. Encarnación-Martínez et al. (2021) found that equations like these predicted optimal knee angles for 47-60% of males and 20-33% of females. Females also have a lower foot-to-inseam ratio (24.4% vs 25.1%), affecting pedal leverage and causing overestimation of saddle height, which can lead to over-extension of the knee (Encarnación-Martínez et al., 2021). This under-representation extends into other areas of cycling modelling literature. Ettema et al. (2009) derived joint-power parameters from male-only cohorts and Heil (2001) developed frontal area scaling laws from male competitive cyclists, with neither being validated against female anatomy. Hoffmann

et al. (2024) confirmed that minimising angular jerk is a primary kinematic optimisation, but the movement strategies to achieve this differ between sexes, undermining direct transferability of models which only observe kinematic outcomes.

2.3 Sex-specific Anatomy and Biomechanical Consequences

The under-performance of fitting equations for female cyclists is validated by anatomical differences that industry "shrink and pink" practices fail to accommodate (Dixon et al., 2017).

2.3.1 Skeletal Differences. Female pelvic geometry is significantly different from males with a wider ischial tuberosity (135.3mm vs 114.0mm) and broader pubic arch angle ($> 90°$ vs. $< 90°$), affecting saddle interactions and posture (de Vey Mestdagh, 1998; Potter et al., 2008; Carpes et al., 2010). Females also have shorter arm-to-leg ratios (1.49 vs 1.52) and typically have a femur 1cm longer for a given leg length, impacting knee alignment and effective reach (Lin et al., 2023). A wider pelvis can increase Q-angle, raising the risk of dynamic knee valgus when pedal stance width is fixed (Kotler, 2023).

2.3.2 Saddle Interface and Pressure Distribution. When female cyclists adopt forward pelvic tilt (encouraged for aerodynamics and power levels), the wider pubic arch places disproportionate pressure on the pubic symphysis rather than the ischial tuberosities (Potter et al., 2008; Baran et al., 2014). Such anterior loading compresses the pudendal nerve and artery, raising risk of sexual dysfunction and numbness. Larsen et al. (2018) found that factors such as saddle nose width and cutout design significantly alter pressure distribution in female cyclists. Lin et al. (2023) demonstrated that to mitigate such anterior loading a saddle should be at least 1cm wider than the ischial tuberosities, which is noted to be a requirement rarely met by standard equipment.

2.3.3 Kinematic Divergence Under Load. Vicari et al. (2025) found that as pedalling intensity increases, males increase anterior pelvic tilt in order to engage gluteal muscles, whereas females shift weight posteriorly. Potter et al. (2008) found this posterior shift (adopted to relieve saddle discomfort) actually reduces gluteal activation, decreasing power output. These adaptations can result in perineal trauma, persistent discomfort and neuromuscular inefficiencies linked to gluteal activation patterns (Potter et al., 2008; Dettori and Norvell, 2006). The kinematic divergence has not yet been quantified through simultaneous neuromuscular and metabolic measurement, which this study aims to address.

2.4 Measurement Technologies

2.4.1 Motion Capture. 2D camera motion-capture (mo-cap), still common in professional fitting, underestimates knee flexion by 2.2° relative to 3D systems, a significant gap when this is one of the critical variables analysed (Fonda et al., 2014). Marker-based systems including Qualisys and Vicon remain "gold standard" (Liparoti et al., 2020), but can introduce soft tissue errors, especially at the pelvis (Wangerin et al., 2007) as well as being more intrusive for participants.

Markerless deep-learning systems offer a practical balance for mo-cap in research. Sagittal plane validity is high ($RMSD < 6°$) (Wren et al., 2023; Kearney et al., 2025), and Chung et al. (2019) demonstrated high validity for upper body joint tracking ($CMC > 0.9$). However, some documented limitations include: underestimation of hip flexion by 14° (Harsted et al., 2019), errors in wrist and rotational tracking (Chung et al., 2019), segment overlap challenges (Ceseracciu et al., 2014) and lower accuracy during non-standard movement patterns (Horsak et al., 2023), which may be relevant for novice cyclists. The deep-learning system used in this study (Theia3D) is designed to tackle occlusion challenges, with D'Souza et al. (2024) providing validation.

To address rotational limitations of camera-based mo-cap systems, Inertial Measurement Units (IMUs) can provide pelvic and spinal orientation data. Peeters et al. (2021) found strong correlations between IMU-derived spine angles and projected frontal area, validating potential use for drag estimation. The implication for this study is that IMU-derived spinal acceleration can substitute for full-body kinematic data when motion-capture coverage is partial, providing a postural-change signal independent of the strain/pressure redistribution signals.

2.4.2 Neuromuscular Assessments through EMG. Chapman et al. (2009) observed that novice and elite cyclists can display indistinguishable lower-body joint angles while having substantially differing muscle recruitment patterns, suggesting kinematic data alone is insufficient to optimise for physiological efficiency. Chapman et al. (2008) identified co-contraction (muscles working against each other) as a primary marker of inefficiency only detectable through EMG. Zakaria et al. (1996) reported good reliability for absolute integrated EMG (ICC=0.69-0.89), but lower reliability for inter-muscle ratios (ICC<0.40), supporting use of normalised activation amplitude over ratio-based indices. Normalisation will be crucial as females have greater subcutaneous fat around the gluteal region (Belzunce et al., 2023), so EMG signal amplitude may be reduced.

2.4.3 Metabolic Assessment. Jones et al. (2011) claim the VO_2 slow component is a sensitive indicator of metabolic efficiency, which is a progressive increase in oxygen intake during steady-load exercise caused by fatigued fibre recruitment. Lucía et al. (2000) found elite cyclists have stable VO_2 levels at threshold intensities, while less efficient cyclists show a steady drift. Korzeniewski and Zoladz (2015) showed that fatigue increases ATP cost of force production which means a poor fit can amplify the VO_2 slow component regardless of muscle recruitment, implying that fitting-induced local fatigue can produce significant metabolic penalties.

Near-infrared spectroscopy (NIRS) provides a complementary local data stream through muscle oxygen saturation (SmO_2). Feldmann et al. (2019) established the Moxy monitor provides a valid 0-100% SmO_2 scale across muscle groups that are mirrored in this study. However, signal accuracy is sensitive to adipose tissue thickness, with reliability falling at >15mm. This limitation will likely compound due to the increased gluteal subcutaneous fat that Belzunce et al. (2023) discussed.

2.5 Multi-Modal Data Fusion

Measuring these modalities together introduces analytical complications. Sensor sampling rates range from 0.5Hz (gas exchange) to 1000Hz (sEMG) and metabolic responses lag behind the events that caused them by roughly 12-16 seconds (Procházka et al., 2017). Sample-aligned joins presume zero lag and equal sampling rates, assumptions violated by real data. Although feature-level fusion over fixed windows has been proposed in the literature (Lahat et al., 2015), it remains uncommon in fitting research. Studies integrating sex-stratified cohorts with multi-modal sensing must therefore define their fusion strategy as a critical design decision.

Millour et al. (2023) argue that any particular data stream cannot suffice for an assessment of positional cost of cycling, and the relationship between movement stability and metabolic efficiency can only be found through concurrent multi-modal sensors. This is supported by the previous section: kinematic data fails to capture neuromuscular inefficiency (Chapman et al., 2009), EMG cannot capture metabolic cost, metabolic cost cannot localise inefficiency.

Simultaneous sensor recording introduces the registration problem (Lahat et al., 2015), which is the fusing of data with different sampling rates. These will range from EMG signals up to 1259Hz to breath-by-breath gas exchange below 1Hz. Katmah et al. (2023) reviewed fusion approaches for asynchronous signals and recommended feature-level fusion. This involves extracting metrics such as mean EMG RMS, peak knee angle or VO_2 slope before integration, avoiding sample-by-sample temporal alignment.

Procházka et al. (2017) demonstrated a 12-16 second physiological lag between load changes and metabolic response, consistent with broader findings on physiological response timings (Atkinson et al., 2007). Cross-correlation or time-shifting methods may therefore be needed to attribute metabolic cost to the event that produced it. Wu et al. (2020) demonstrated that transforming physiological time series into engineered summary features can achieve high prediction accuracy ($R^2 = 0.979$), outperforming raw-signal approaches.

2.6 Computational Modelling

Traditional statistical tests identify differences between groups but might miss complex, non-linear relationships between biomechanical and physiological variables. Bing et al. (2025) achieved 99.79% accuracy classifying saddle heights using KNN, acknowledging that the model lacked generalisability with the absence of sex stratification, noting different joint angles may be present at equivalent saddle heights.

Through training of separate classifiers for each sex and comparing feature importance, one could determine whether the biomechanical features that distinguish well-fitted from poorly-fitted are different for males and females. Such classifiers may require neuromuscular features to detect maladaption, reflecting the 'invisible' kinematic compensatory patterns described by Potter et al. (2008); Chapman et al. (2009); Wu et al. (2020).

2.7 Summary

Current bike fitting protocols systematically underperform on female cyclists as they have been formulated on equations derived predominantly from males. This means that anatomical differences such as pelvic geometry, limb proportions and saddle interface can produce kinematic compensations e.g. posterior pelvic shift or reduced gluteal activation, of which the physiological cost has not been fully quantified. Evidence that kinematic similarity can hide muscular divergence (Chapman et al., 2009) shows that concurrent multi-modal data is necessary to measure these potential maladaptions.

This review of the literature as well as the RQs for the project have led to the following hypotheses (all linked to their respective RQs):

H1: Analysis will detect significant pre-to-post fit changes in **at least 5** outcome variables in a unified feature matrix, surviving Benjamini-Hochberg correction at $q < 0.05$.

H2: Condition × sex interactions will be significant for saddle pressure and gluteal-EMG change scores, with females showing a greater $|d_z|$ than males due to compensatory strategies described by Potter et al. (2008); Vicari et al. (2025).

H3: A random forest classifier will assign higher feature importance to neuromuscular features than kinematic features, in line with Chapman et al. (2009)'s findings.

H4: Pre-to-post change scores will show at least one cross-modal Spearman correlation of $|r_s| \geq 0.35$ excluding within-modality blocks, and correlation structure will differ between sex-stratified sub-samples.

This study addresses these gaps by collecting synchronised kinematic, neuromuscular, metabolic and pressure data from 51 cyclists stratified by sex and experience, before and after professional bike fit. A feature-level fusion pipeline resolves the registration problem across asynchronous signals, enabling analysis of variables that have previously been studied in isolation. Sex-stratified comparisons will quantify responses to fitting. Feature importance analysis will allow exploration of variables to see if those that distinguish from a well-fitted to a poorly-fitted setup changed between sexes, and whether neuromuscular features are required to detect maladaption that kinematic measures alone may miss.

3 System Design

3.1 Participants and Recruitment

51 cyclists were recruited through university sports group chats, primarily through cycling and triathlon. The rowing club was also used to gain participants with limited cycling experience but strong aerobic bases. All participants were aged 18 or over and free from musculoskeletal injury, cardiovascular contraindications, or neurological conditions likely to alter movement patterns. Ethics approval was granted (14477-17122) and all participants provided informed consent prior to participation.

Participants were grouped by sex and self-reported cycling experience. This was motivated by Chapman et al. (2009)'s findings that experience level modulates muscular recruitment independently of

kinematics. A power analysis determined a target size of 25 participants per group. At the data collection cut-off for this paper, all 51 participants had completed sessions 1 and 2, while 36 had completed session 3. Analysis of pre-vs-post fit are therefore primarily based on the 36 participants who completed all 3 sessions, but all data will be analysed. The final sample consisted of 27 males and 24 females. Experience was defined such that participants who spent more than 2 hours a week cycling (including static bikes) would be classified as experienced, which produced a count of 25 experienced and 26 non-experienced.

3.2 Protocol overview

Data collection included three lab sessions. The majority of participants completed these sessions in numerical order as this best reflected the real world sequence of perform, fit, perform. Due to scheduling constraints and pilot sessions, 4 participants completed session 3 before session 2. Participants were instructed to abstain from caffeine, alcohol and vigorous exercise in the 24 hours preceding each session.

3.3 Session 1: Baseline Assessments and self-selected fit

On arrival, resting heart rate was assessed using a chest strap. Participants rested quietly for 5 minutes before 5 minutes of monitoring, providing a cardiovascular reference against which session-specific exertion could be contextualised. Anthropometric measurements were then collected, including height, body mass, leg length, torso length, arm length and foot size. These would inform initial bike configurations and provide variables for biomechanical modelling.

The Wahoo KICKR bike was initially configured using the following setup. Crank length was fixed at 170mm to eliminate it as a confounding variable. 170mm was used because Li et al. (2025) found this length reduced subjective fatigue and acted as an optimal balance for well-trained amateurs who value both comfort and power output. Saddle height was set using the LeMond method, calculated as inside leg length multiplied by 0.883 (Encarnación-Martínez et al., 2021). Saddle fore-aft was then set such that when the pedal was at the furthest anterior position the knee would lay directly above the pedal axle. Handlebars were initially set level with the saddle, adjusting reach so that the angle between arms and torso would be roughly 90° when hands were placed on the hoods. This initial setup was such that non-experienced cyclists wouldn't adapt a bad position without knowledge of what an optimised setup would feel like. Participants were then encouraged to adjust anything that would make the fit more comfortable, which would then be recorded as their baseline setup.

Participants completed a ramp test to estimate Functional Threshold Power (FTP). The test used erg mode on the KICKR bike, where power is controlled independently of cadence. Male participants started at 100W while female participants started at 75W, with power increasing 25W every minute until failure. When a participant stopped pedalling mid-interval, the final power value was linearly interpolated. FTP was estimated at 75% of peak power (Allen and Coggan, 2010).

3.4 Session 2: Self-fitted Performance Trial

For session 2, the bike was mirrored to the setup used in session 1, allowing adjustments if the participant was uncomfortable. Sensors were applied according to the protocol described in section 3.6. Participants were allowed to warm up however they liked before beginning a 20 minute trial at the estimated FTP from session 1 (using erg mode again for power control). Subjective effort was recorded at 4, 9, 14 and 19 minutes using a Rating of Perceived Exertion (RPE) scale from 0 (rest) to 10 (maximal) in intervals of 0.5. If participants were unable to sustain power or gave an RPE of 9.5/10 (excluding the reading at 19 minutes), output was managed by reducing wattage by 5% of the initial target. Following the trial, heart rate was monitored until it returned below 100bpm.

3.5 Session 3: Fitted Performance Trial

Session 3 began with a professional bike fitting, followed by a repeat of the session 2 performance trial. The bike was initially set to the configuration from previous sessions and then our fitter performed a comparative fitting assessment, adjusting saddle height, saddle setback, handlebar reach, handlebar height, seat angle and crank length to optimise for both comfort and power output. Cleat position, saddle angle, inner shoe wedges, bar width and hood position were not adjusted during the fit, defining the fit as gross road positioning only (Corke, 2026). The new configuration was recorded before sensor application and the performance trial. The trial was completed at the lowest wattage used in the session 2 trial.

3.6 Sensor Instrumentation

The multi-modal sensor suite is shown in Table 1. 16 Delsys Trigno sensors recorded surface electromyography (sEMG, measuring muscle recruitment) at 1259Hz and IMU data (accelerometer and gyroscope) at 148Hz from bilateral lower limb and unilateral upper body muscles, positioned according to SENIAM advice (Challis, 2021). 8 Moxy NIRS sensors provided muscle oxygen saturation and total haemoglobin measurements. A COSMED K5 recorded breath-by-breath VO_2, VCO_2 and RER via a respiratory mask. Three-dimensional joint angles and skeletal structures were captured using both IRIS (a motion capture system developed by the Impact Team) and Qualisys markerless motion capture systems, using Theia3D to post-process. Saddle, handlebars and removable shoe insoles had pressure sensors, with strain gauges also being present on the seatpost and stem (designed by the hardware team, see appendix M for further details). Power output and cadence were recorded via the KICKR bike's onboard power meter, supplemented by Garmin power-pedals. Heart rate was recorded with a Garmin chest strap, with a custom board measuring tidal flow. See Figure 8 in Appendix F for the physical camera layout used during capture.

See Figure 7 in Appendix B for visualisation of Trigno and Moxy sensors locations.

3.7 System Integration and Data Collection Efforts

Integrating the sensor suite into a single capture session was a principal experimental challenge. The Bikefit web platform, Delsys Trigno EMG/IMU, Moxy NIRS, COSMED K5, Qualisys/Theia3D markerless capture, IRIS, strain-gauged seatpost and handlebars,

Table 1. Consolidated Technical Architecture of Heterogeneous Sensor Streams

Sensor / System	Key Metrics	Placement Scope (Condensed)
Delsys Trigno (x16)	sEMG (1259Hz), IMU	Bilateral (B): VL, RF, Hams, GMax, Gastroc., TibAnt. Left (L): ES, Lats, Delt.
Moxy NIRS (x8)	SmO2, Total Hemoglobin	B: Vastus Lat, Glute Max, Biceps Fem, Med Gastroc.
Cosmed K5	VO2, VCO2, RER	Respiratory mask (breath-by-breath analysis).
IRIS (4 webcams) & Qualisys (8 markerless)	3D Joint Angles, θ	Full-body markerless skeletal tracking.
Strain Gauges, Pressure sensors	Force (N), Pressure	Static Interfaces: Handlebars, Saddle, Footbed.
Garmin / Bike	Watts, Cadence	Crankset and Pedal-based ANT+ feeds.

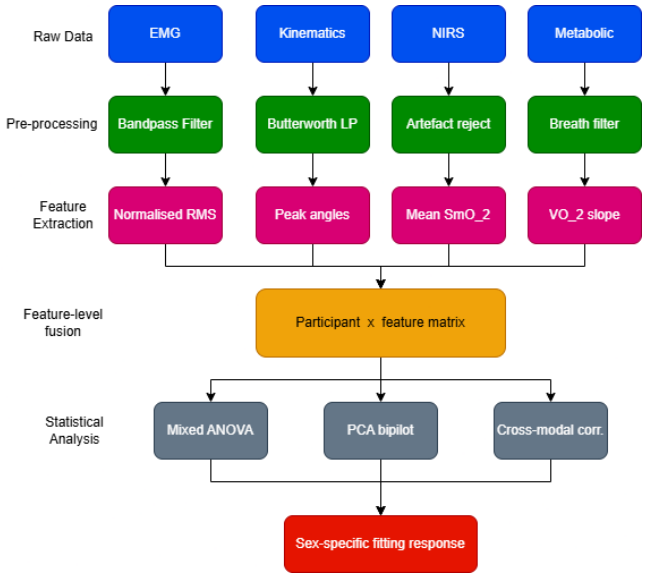


Fig. 2. Flow diagram of data

insole pressure boards and the Wahoo KICKR each ran on independent clocks, sampling rates and start-up sequences. We iterated through three primary pilot tests to identify any potential issues, each leading to updates in our pre-session checklist. Two trained researchers were required to apply sensors in parallel in a given session window.

Lab session 1 was scheduled for 60 minutes, session 2 for 90 minutes and session 3 for 120 minutes with each day requiring approximately 45 minutes of preparation time (primarily to allow COSMED to warm up). Across eight weeks of data collection, six days a week, we ran 138 sessions, totalling 13,410 minutes (223.5 hours) of testing. Both primary researchers did around 200 hours of data collection as well as training additional researchers to continue data collection after our internal cut-off. When accounting for familiarisation with the hard- and software stack, participant scheduling, experimental planning and team meetings this study took in excess of 250 hours of researcher time before data processing and analysis could begin.

4 Evaluation Method

4.1 Preprocessing

Demographic data was exported from the MS form as a spreadsheet with ~28 columns per participant (including some irrelevant metadata), identifying data such as names/emails were dropped before analysis. Anthropometric fields were converted to floats, DoB was compared against the form submission time to derive age. Free-text responses (ranges such as "1–2" or qualitative entries such as "none") were resolved to numeric values using a regex parser. Resting heart rate sometimes had implausible readings, so all readings are assigned a binary tag verifying reliability. Shoe sizes were converted to EU sizing, which was sex aware, due to inconsistent reporting of UK/EU sizing. FTP/kg was derived from the initial ramp test figures. There were also sanity checks for data to be inside of plausible ranges e.g. resting hr 30-100, FTP 50-500. The resulting participant table acts as the join key for subsequent notebooks.

RPE ratings were exported from an Excel spreadsheet. Manual header assignment used a hard-coded column list to encode the layout, producing a per-participant per-session time point row. Any values outside of the 0-10 range were discarded and power drops were parsed, also flagging those trials that had to have power reduced.

COSMED exports begin with a metadata header including: test date, barometric pressure, ambient temperature, humidity and STPD correction factor before the breath-by-breath times series. Header extraction was row-indexed, and the data start row was identified by scanning column J for the first `time` object, as the header was not consistent between all files. Time values are normalised to seconds from the start point. A session was marked as fully complete if it lasted over 1100 seconds, with incomplete tests being flagged. Mean values were computed over four 5-minute epochs (0-5,5-10,10-15,15-20 minutes) and a last 5-minute window, producing wide-format columns for Rf, VT, VE, VO_2, VCO_2, RQ, VO_2/kg, VE/VO_2, VE/VCO_2, $PetCO_2$, energy expenditure, fat/carbohydrate oxidation and cadence. The last 5-minute window was used to approximate steady state responses while also remaining sensitive to VO_2 slow-component drift across the trial (Jones et al., 2011; Baran et al., 2014).

Kinematic data was collected with an eight-camera Qualysis setup (see Figure 8 in Appendix F) and processed through Theia3D to estimate markerless positions at 100Hz. Each session provided a JSON of body segments, each of which comprised of flattened 4×4 homogenous transformation matrices. While these are parsed, invalid frames are forward filled and reshaped to (N, 4, 4) arrays. For 18 joint pairs relative rotation was computed and yaw, pitch and roll were extracted, producing 54 joint-angle columns per frame. A zero-phase 4th-order Butterworth low pass at 6Hz was applied to preserve pedalling cadence and its harmonics while removing

high-frequency jitter (Kearney et al., 2025; Wren et al., 2023). Top-centre events were detected as the minima of right knee flexion. Cycles outside the range of 60-150RPM as well as the first and last 60 seconds of the trial were all discarded, ensuring that initial leg speed builds and finishing sprints would not affect averages. Remaining cycles were partitioned into 36 crank angle bins of 10°, with the mean joint angle per bin per participant recorded. Qualysis TSV timing files allowed the Theia3D frame counter to be anchored, ensuring alignment with other sensor streams.

Trigno sensors transmit surface **EMG** (1259Hz) with tri-axial accelerometer and gyroscope (148Hz) channels in a single packet, extracted in the same loop iteration. Sensor IDs are mapped to certain muscles through `config.yaml`, with overrides for occasional use of backup sensors.

The EMG envelope pipeline includes: z-scoring (remove DC offset and inter-electrode gain differences), 4th-order zero-phase Butterworth high-pass at 5Hz (remove pedalling frequency artefact); full-wave rectification, and a 4th order zero-phase Butterworth low-pass at 20Hz (to produce a smooth linear envelope). Signals were not min-max normalised, preserving cross-section recruitment ratios (Zakaria et al., 1996). IMU preprocessing produced per-axis means and the vector RMS. RMS of acceleration magnitude was used as a stability proxy for the lower back sensor, providing potential insight into drag-posture coupling (Peeters et al., 2021).

Moxy NIRS packets are identified by MAC addresses of sensors, with the final four digits mapped through IDs in `config.yaml`. Stats produced include: SmO_2 and total Haemoglobin (per position). **Pressure sensors** supply a 20×20 $matrix$ per packet, accumulated to a running mean to produce an average pressure map, allowing centre of mass calculations. **Strain gauges** exhibit session-specific baselines due to environmental differences such as temperature drift. Values are normalised by subtracting the 1st percentile of the full-session signal, leading values to report load above rest. Samples exceeding $\pm 5 \times IQR$ from the median are dropped as spikes. The respiration belt mirrors this, recording: last 5-minute mean, RMS and peak-to-peak summary. Bike and heart-rate streams are filtered to standard ranges to avoid recording spikes (0-1500W, 30-220bpm) and averaged over the final 5-minutes. Pedal balance (when power pedals were used, not everyone had cleats) was converted to an asymmetry index $|B - 50| \times 2$.

4.2 Feature Extraction

Each session was represented by a row of a unified feature matrix. Features fell into five groups:

Metabolic features capture aerobic cost and drift: last 5-min VO_2/kg, VE, VCO_2, RQ, ventilatory equivalents, energy expenditure, fat/carbohydrate oxidation rates and the VO_2 slow component slope, computed from a linear regression of VO_2 across 5-20 minutes (Jones et al., 2011). Gross efficiency was computed as $(MechanicalPower \times 60)/(netVO_2 \times 20.9kJ/L) \times 100$, using the final 5 minutes to approximate steady state.

Neuromuscular features summarise muscle recruitment at individual sites. Last-5-min mean EMG readings are extracted and a co-contraction index in the format of Chapman et al. (2008)'s was computed for the primary antagonist pairs (quadriceps-hamstring and tibialis anterior-medial gastrocnemius) as $CCI = (2min(a, b)/(a + b)) \times 100$. This was extended with per-site Moxy SmO_2 and tHb for local oxygen utilisation.

Kinematic features are extracted from the crank cycle resolved joint angles that are produced in NB4. These include mean/peak flexion per cycle, range of motion, joint angles of the hip, knee, ankle and trunk when the crank was at the top.

Bike and pedal features comprised last 5-min mean power, cadence, heart rate and pedal left-right asymmetry index.

Subjective Features are the RPE readings at 4,9,14 and 19 minutes, mean RPE at those timestamps and a binary `power_drop_before` flag.

4.3 Feature-level fusion

A resulting feature matrix has one row per participant per session over roughly 150 columns. Missing values are augmented with column mean and all features are standardised to zero-mean and unit variance before analysis. Delta scores $\Delta = Session3 - Session2$ are computed per participant for every feature to form the basis of H2 and H4 analysis.

Cross-correlation between cadence and heart rate time series at lags of 0-30 seconds recorded peak correlation lag per session. The produced lag distribution justifies feature-level fusion (over sample-level) as a fixed sample-aligned join would attribute metabolic responses to the incorrect event causing them when lag varies between participants.

4.4 Inferential statistics

Hypothesis tests were summarised and reported with both raw p-values and Benjamini-Hochberg FDR-corrected q-values. Normality was assessed per cell with Shapiro-Wilk. As >50% of cells violate the normality assumption Wilcoxon signed-rank (within-sex) and Mann-Whitney U (between-sex) are adopted as primary tests. Effect sizes are reported with p-values and magnitude classifications applied. Percentile bootstrap 95% confidence intervals (with n=2000 resamples) are computed for sex differences in change scores across key outcome variables.

H1 was tested via paired Wilcoxon signed-rank on every feature, with Benjamini–Hochberg FDR correction applied within the H1 matrix (Figure 3). H2 was tested with a 2×2 mixed ANOVA per dependent variable using `pingouin.mixed_anova`, using sessions as the within-subjects factor and sex as the between subject factor. Saddle pressure was examined for H2 including centre of pressure, left-right asymmetry and contact area derived from the 20×20 map, tested between and within sex. Gluteal activation was tested using the EMG envelopes relevant to that area. An additional three-way ANOVA (using cycling experience as an additional between-subjects factor) was reported, but with ~ 12 participants per cell it was underpowered for three-way interactions, so effect sizes are used over p-values for that analysis.

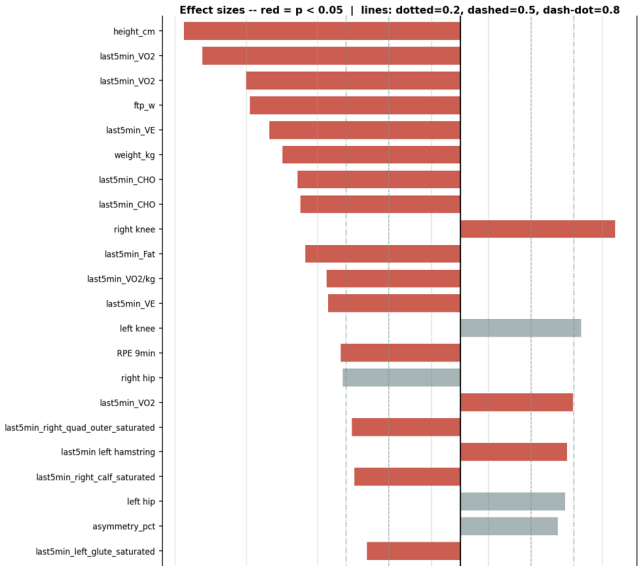


Fig. 3. Forest plot of paired effect sizes (Cohen's d_z, S3−S2) for top 22 features in the unified matrix, with 95% bootstrap confidence intervals (n = 2000 resamples). Markers right of zero favour the fitter-adjusted condition. Red labels denote Benjamini–Hochberg FDR survivors at $q < .05$. Abbreviated view; full numeric table in Appendix HTable ??.

4.5 Explanatory multi-modal analysis

H3/H4 are explored through analysis on the feature matrix. A PCA biplot of features serves as an initial descriptive diagnostic. Cross-modal Spearman correlations between pairs of change-score features are then computed. For H3, `RandomForestClassifier` with 500 trees, balanced class weight and LOSO validation, was trained separately on sex-specific subsets to classify self selected vs. fitter selected condition. The primary output for the classifier was feature importance ranking. Each feature was assigned a modality group and mean importance per modality was computed for each classifier. A one-sided Mann-Whitney U tests the prediction that neuromuscular importance exceeds kinematic importance, motivated by Chapman et al. (2009).

5 Results

5.1 Sample Characteristics and Data Completeness

Of the 51 participants (24 female, 27 male; 25 experienced, 26 inexperienced), all completed the 20 minute self-fitted trial (session 2). 36 participants (15 female, 21 male) completed the professionally-fitted trial (due to data collection time restraints); this subset forms the paired sample used for H1, H2 and H4, with the remaining 15 participants contributing to descriptive statistics only. Sexes were well-matched for age ($p = .92$) and reported cycling volume ($p = .87$), but expectedly differed on anthropometry and absolute power (Table 9). Males were taller (+15.0 cm, $d = -1.94$), heavier (+16.3 kg, $d = -1.25$) and produced higher FTP (+79.5 W, $d = -1.47$), with an advantage in relative power (+0.42 W kg^{-1}, $d = -0.63$, $p = .046$ uncorrected but non-significant after FDR).

Of the 87 20-minute trials completed, 85 satisfied duration, heart-rate, power-stability and sensor completeness criteria simultaneously. EMG delivered all channels in 85 sessions, NIRS in 80 and gas exchange in 86. Insole pressure sensors only produced usable data in 36 sessions (see Section 6.9), so H2's analysis depends on saddle pressure and seatpost/handlebar strain gauges. A full per-session data checklist appears in Appendix H Table 10.

5.2 Cohort response to fit

Pre-to-post fit changes were tested using a paired Wilcoxon signed-rank for every feature and Benjamini-Hochberg FDR-corrected values (Appendix Table 13, Appendix Figure 24). Two variables survived correction at $q < .05$: VCO_2 ($\Delta = +163.8$ ml min^{-1}, $d_z = +0.43$, $p_{FDR} = .024$) and the left medial gastrocnemius (calf) sEMG ($\Delta = -0.04$ NU, $d_z = -0.56$, $p_{FDR} = .024$). An additional five metabolic variables fell in the $.05 < q < .11$ range: VO_2 kg^{-1} ($d_z = +0.46$), tidal volume V_T ($d_z = +0.49$), energy expenditure ($d_z = +0.39$), heart rate ($d_z = -0.35$) and right-calf SmO_2 ($d_z = -0.37$). Matched direction of change over VCO_2, VO_2, V_T and energy expenditure paired with a decrease in heart rate suggests the fit shifted participants to a more ventilation-led and less cardiovascular strained condition. 19-min RPE did not move at the cohort level (all four paired comparisons $q > .37$), implying that the metabolic shift was not subjectively noticeable within a single trial. H1 is therefore partially supported.

Table 2. H1 pre-/post-fit paired effects (n = 36 cyclists, S3−S2). Features ranked by uncorrected p; only those with uncorrected $p < 0.10$ are shown. Full results in Appendix Table 13. d_z is Cohen's d for paired data.

Modality	Variable	M_{S2}	M_{S3}	d_z	p / p_{FDR}
COSMED	VCO_2 (ml min^{-1})	3018.7	3182.6	+0.43	.001 / **.024***
EMG	L. calf (NU)	0.595	0.553	−0.56	.001 / **.024***
COSMED	VO_2 kg^{-1}	41.88	47.06	+0.46	.003 / .053
COSMED	V_T (L)	2.10	2.22	+0.49	.005 / .053
COSMED	EE (kcal)	21466	23987	+0.39	.005 / .053
Bike	Heart rate (bpm)	173.2	162.0	−0.35	.010 / .086
Moxy	R. calf SmO_2 (%)	43.66	36.24	−0.37	.013 / .100
COSMED	VO_2 (ml min^{-1})	3204.9	3373.5	+0.38	.016 / .108
EMG	R. lower back	0.586	0.654	+0.36	.041 / .221
RPE	RPE at 9 min	7.42	6.92	−0.36	.041 / .221
Moxy	R. glute SmO_2	45.62	54.17	+0.41	.050 / .244

* survives Benjamini-Hochberg FDR at $q < .05$; ** $q < .01$.

Measurable postural changes accompanied this metabolic shift. Lower back IMU acceleration decreased on the superior-inferior axis ($d_z = -0.51$, $p_{FDR} = .004$) and rose on the anteroposterior axis ($d_z = 0.39$, $p_{FDR} = .039$), consistent with a forward trunk pitch and reduced bounce, a redistribution fitters often target (Millour et al., 2023). Saddle and handlebar strain gauges validate this redistribution, showing that total saddle force decreased by 21.8 kN·samples ($d_z = -0.90$, $p < .001$), centre-of-pressure shifted posteriorly by 4.5 mm ($d_z = +0.85$), seatpost mean load dropped ($d_z = -1.02$) and handlebar mean load rose ($d_z = +0.83$). The forward saddle position therefore unloaded rear strain, redistributing weight onto the handlebars. IMU and strain-gauge data shows a signature of the

standardised fit is the forward and downward shift of rider mass and better trunk stabilisation, allowing metabolic cost to fall.

Table 3. Within-sex paired Wilcoxon tests, S3−S2. Only features with uncorrected $p < 0.05$ in at least one sex are shown. Signs are such that $d_z > 0$ is an increase from S2 to S3.

Group	Variable	d_z	p_{unc}	p_{FDR}
Female	VO_2	+0.79	.010	.104
Female	$VO_2\,kg^{-1}$	+0.62	.010	.104
Female	VE	+0.65	.026	.178
Female	L. hamstring EMG	+0.75	.018	.149
Female	L. calf EMG	−0.56	.035	.187
Female	L. glute SmO_2	−0.65	.049	.187
Female	R. quad outer SmO_2	−0.76	.012	.104
Female	R. calf SmO_2	−0.74	.020	.149
Female	R. quad outer tHgb	−0.62	.035	.187
Male	Heart rate	−0.62	.032	.187
Male	L. calf EMG	−0.54	.016	.149
Male	R. calf EMG	−0.52	.038	.187
Male	RPE at 4 min	−0.48	.033	.187
Male	RPE at 9 min	−0.84	.001	.020
Male	RPE at 19 min	−0.50	.034	.187

Cross-correlating cadence against heart rate per session at lags of 0-30s produced a distribution with modes at 0s and 30s and a median peak correlation of 18s, near the 12-16s range reported by (Procházka et al., 2017). In 46% of sessions the best match occurred at the upper search bound, suggesting true lag may exceed 30s for some participants. The distribution did not differ between sexes (χ^2 on $\{0, 1-29, 30\}$ s bins, $p = .42$). A sample-aligned join would therefore have attributed metabolic response to the incorrect biomechanical events in 80% of trials, supporting the use of feature-level fusion for the pipeline.

5.3 Sex-specific divergence in fit response

Though cohort-level effects appeared modality-balanced, splitting paired tests by sex showed that males and females adapted to the fit via distinct physiological profiles (Table 3). Females displayed the metabolic-uptake profile: VO_2 ($d_z = +0.79, p = .010$), $VO_2\,kg^{-1}$ ($d_z = +0.62, p = .010$), VE ($d_z = +0.65, p = .026$) and left-hamstring sEMG ($d_z = +0.75, p = .018$) all rose, while outer-quadriceps and calf SmO_2 fell ($d_z \leq -0.74$). However, males displayed the cardiovascular-subjective cost profile: heart rate dropped ($d_z = -0.62$), bilateral calf sEMG fell ($d_z \leq -0.52$) and Borg RPE fell at every recorded timepoint (d_z between −0.48 and −0.84). No within-sex effects survived FDR correction, but the strongest signals are RPE-9-min drop for males ($p_{\text{FDR}} = .020$) and right-calf SmO_2 drop for females ($p_{\text{FDR}} = .149$). This asymmetry is lost at the cohort level where female metabolic increases and male cardiac decreases average to a ventilation-led pattern.

This divergence was tested using two-way mixed ANOVAs (condition × sex) on every variable. The interaction term only reached $p < 0.05$ for one variable, end-trial RPE at 19-min ($F_{1,32} = 7.78$, $p = .009$, $\eta_p^2 = .196$), where males dropped 0.575 points (95% CI $[-1.08, -0.10]$) while females rose 0.5 points (95% CI $[+0.04, +1.00]$), giving a between-sex difference-of-deltas of 1.08 points (CI $[-1.79, -0.34]$). This 1 point difference on a 0-10 RPE scale is meaningful for a single session positional change (Bini, 2020), one explanation is that the same forward saddle translation unloads the ischial tuberosities for males while increasing pubic-symphysis pressure for females, due to the broader pubic arch (Larsen et al., 2018; Lin et al., 2023) . VE ($\eta_p^2 = .085$, $p = .084$), left-hamstring sEMG ($\eta_p^2 = .086$, $p = .082$) and right-calf sEMG ($\eta_p^2 = .037$) were all close to significance ($.05 \leq p \leq .10$). This suggests that a single fit protocol can produce equal kinetic redistribution but unequal psychophysical comfort, and in turn perceived effort, across sexes.

Table 4. Session × sex interaction term from 2 × 2 mixed ANOVAs. Only features where either the session main effect or the interaction reached $p < .10$ (uncorrected) are listed. η_p^2: partial eta-squared.

Family	Dependent variable	F	p	η_p^2
Subjective	RPE at 19 min	7.78	.009	.196
EMG	L. hamstring	3.21	.082	.086
COSMED	VE	3.17	.084	.085
EMG	R. calf	1.32	.259	.037
COSMED	RQ	1.35	.254	.038
EMG	L. quad outer	1.41	.244	.040
EMG	R. glute	0.95	.336	.027
COSMED	$VO_2\,kg^{-1}$	0.36	.553	.010
Pedal	Balance asymmetry	-	.036	-

Within-sex splits allow a direct test of H2 (prediction that females will show larger compensatory changes in saddle pressure and gluteal activation). Total saddle force, posterior centre-of-pressure shift, seatpost unload and handlebar loading all reached $|d_z| \approx 0.8 - 1.0$ in both sexes (Table 5), with no saddle-pressure ANOVA interaction term reaching significance. Right-glute SmO_2 rose post-fit at cohort level (+8.5%, $d_z = +0.41$, $p_{\text{unc}} = .05$, did not survive FDR), and right-glute sEMG showed no sex-specific change ($d_z = -0.02$ female, $d_z = -0.52$ male). Sexes did diverge on pedal symmetry indices: females shifted right-side (+0.69 from symmetry) while males shifted toward symmetry (−0.55), giving a between-sex interaction ($p_{\text{int}} = .036$). This suggests that contact points respond comparably to the fit between sexes, but load distribution through the pedal stroke does not, consistent with Potter et al. (2008)'s pelvic-tilt mechanism. H2 is therefore not supported.

Two random-forest classifiers were trained separately on sex-specific data to predict if the session was pre or post-fit. These classifiers provided modality-aggregated Gini importance scores reported in Table 6 and Figure 4 to help with importance analysis for H3. Both models are neuromuscular-dominated, but the female classifier weighted EMG features more heavily (62.5% of total importance) than the male classifier (55.1%), and had a substantially lower relative rank of the VO_2 slope (rank 4 male, rank 19 female). The 3 features with the largest (female–male) importance differences were the left hamstring sEMG (+0.052), right glute sEMG (+0.026) and $VO_2\,kg^{-1}$ (+0.032). The three largest (male– female) differences were the VO_2 slope (+0.033), left shin sEMG (+0.037) and right lower-back sEMG (+0.019). Hamstring and gluteal prominence in

Table 5. Saddle pressure and bike-frame strain changes (S3−S2). Δ and d_z reported; p-values from paired Wilcoxon; Bike/Handlebar p-values FDR-corrected within the strain-gauge family.

Sensor	Metric	Group	Δ	d_z	p
Saddle	Total force	All	−21777	−0.90	<.001
Saddle	Total force	Female	−12117	−0.93	.005
Saddle	Total force	Male	−28678	−1.02	<.001
Saddle	COP_y (posterior)	All	+0.45	+0.85	<.001
Saddle	COP_y	Female	+0.39	+1.04	.003
Saddle	COP_y	Male	+0.49	+0.79	.004
Seatpost	S1 mean load	All	−386	−1.02	<.001
Handlebar	S1 mean load	All	+26.6	+0.83	<.001
Handlebar	S1 mean load	Female	+17.2	+0.74	.017
Handlebar	S1 mean load	Male	+32.9	+0.91	.001

the female model is consistent with compensatory strategies described by Potter et al. (2008), and the absence from the top of the male model supports the argument that fit quality cannot be diagnosed off kinematic data alone (H3, supported descriptively).

Table 6. Summed random-forest feature importance by modality and sex; number of features per modality in parentheses. Relative weight: share of total forest importance attributable to that modality.

Modality (n features)	Female (%)	Male (%)
Neuromuscular / EMG (15)	62.5	55.1
Metabolic (VO_2/kg, RQ, VO_2 slope, VE) (4)	17.4	19.2
Mechanical (bike power, cadence) (2)	7.2	7.5
Subjective (RPE at 19 min) (1)	3.6	4.1
Other (VE residual) (1)	3.6	4.2

Values rescale to sum of 100% per column within the displayed columns; slight rounding means column totals may differ from 100 by ±0.3.

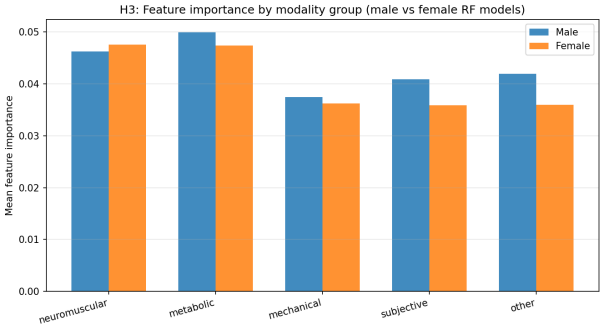


Fig. 4. Random-forest feature-importance aggregated by sensor modality for the S2-vs-S3 classification task, pooled and sex-stratified. Neuromuscular features (EMG) account for 55-63% of the total importance mass. Full per-feature breakdown in Appendix Table 17 and Figure 36.

5.4 Cross-modal coupling of change scores

Spearman correlations between paired Δ-scores (S3−S2) produced 12 pairs where $|r_s| \geq 0.35$ (Appendix HTable 16, full heatmap Appendix HFigure 33). EMG pairs dominated, highlighting the bilaterally symmetric muscle recruitment, but cross modal couplings were the most revealing. Change in mass-normalised metabolic uptake was positively coupled to change in left-hamstring EMG ($r_s = +0.47$), meaning cyclists whose hamstring activation increased post-fit moved towards a more oxidative metabolic profile. ΔRQ was negatively coupled to $\Delta VO_2\,kg^{-1}$ ($r_s = -0.45$), consistent with increased hamstring use recruiting type 1 (slow-twitch) fibres and shifting the oxidative-glycolytic balance (Rouffet and Hautier, 2008). ΔVE tracked ΔRPE at 19 min ($r_s = +0.36$) while neither tracked Δbike power (near-constant), suggesting that the subjective cost of the fit was due to ventilation changes rather than mechanical load. Session 2 and 3 correlation matrices (Appendix Figures 34, 35) show similar structures, meaning we did not find sex specific evidence for cross-modal adaptation differences. H4 is therefore partially supported as cross-modal correlations exist and are physiologically interpretable, but structure does not differ between sexes.

Table 7. Hypothesis outcomes.

Hypothesis	Prediction	Outcome
H1	Professional fit produces significant pre/post changes across multiple outcome variables	**Partially supported.** VCO_2 and left-calf EMG survive FDR, five further metabolic variables fall in the .05-.11 FDR band.
H2	Condition × sex interaction will show larger magnitude changes in saddle pressure and gluteal activations in females	**Not supported as stated.** Saddle total force and posterior COP shift are **non-sex-specific**. Gluteal activation did not change significantly in either sex (although gluteal sEMG data was unilateral, see Section 6.9. The clearest sex interaction was in RPE at 19 minutes ($\eta_p^2 = .20$, $p = .009$) and in pedal-asymmetry delta.
H3	Neuromuscular features are more important than kinematic features for distinguishing fit quality	**Supported descriptively.** Neuromuscular modalities carry 55-63% of RF importance. The female classifier is more neuromuscular-weighted than the male classifier.
H4	Change-score correlations are non-trivial across modalities and differ by sex	**Partially supported.** Twelve cross-modal correlations with $\|r_s\| \geq 0.35$; ΔVE-ΔRPE and ΔVO_2/kg-Δhamstring EMG link physiology to neuromuscular recruitment. Session-level correlation matrices do not clearly differ by sex.

6 Discussion

6.1 Principal findings

A standardised IBFI level-4 gross-road positioning fit, led to a cohort level ventilation-led metabolic shift, reduced cardiac strain and increased trunk stability. Predicted female specific adaptations in saddle pressure and gluteal activation were **not** observed: saddle force redistribution, posterior CoP shift and handlebar loading were similar in magnitude across sexes. The largest sex×session interaction was subjective effort at 19 minutes and pedal-asymmetry delta. Random forest classifiers trained separately on sex-specific data showed a strong neuromuscular importance, highlighting different key muscles in each model. Cross-modal Δscores linked ventilation to RPE and oxygen uptake to hamstring activation, but did not support sex-specific differences in coupling structures.

6.2 A ventilation-led efficiency signature (H1)

H1 was partially supported. The pattern of near-significant effects was consistent and physiologically interpretable: VO_2, VCO_2, tidal volume and energy expenditure increased post-fit while heart rate fell by ~11 bpm. This increase in ventilatory volume combined with cardiac unloading resembles a ventilation-led compensatory profile in response to position changes that open the thoracic cavity and reduce hip/shoulder flexion (Fintelman et al., 2015). The reduction in left-calf sEMG (which did survive FDR) is consistent with a reduction in ankle-dorsiflexor co-contraction as the post-fit saddle/cleat alignment loads the gastrocnemius less (Bini et al., 2010). Gross efficiency showed no systematic change, matching suggestions that single-fit interventions rarely produce large efficiency gains in a short term period (Martin and Brown, 2009) and that improvements may be longer term and perceptual (Priego Quesada et al., 2019; Bini, 2020).

IMU data gives additional evidence that the fit produced measurable posture change. A drop in lower-back vertical acceleration matched with an anteroposterior increase is consistent with a forward-pitched torso and reduced trunk bounce, a common aspect that fits try to address, see Table 2 (Millour et al., 2023). The complete set of full body kinematic angles from Theia3D had not finished processing at the time of writing, meaning the H3 feature matrix relies on IMUs as a kinematic proxy. This cohort-level signature is the average of two distinct sex-specific responses, discussed in the next section.

6.3 Sex-divergent response profiles: re-framing H2

One of the strongest interpretive findings was that H2 was **not** supported. We had predicted females would have larger changes in saddle pressure and gluteal activation than males. Data showed that saddle total force reduction, posterior CoP shift, handlebar-load increase and seatpost-load reduction were not sex-specific, with effect sizes of comparitively large changes in both groups and no significant change in sEMG between sexes (Table 5). Potter et al. (2008)'s proposed mechanism, where forward pelvic tilt → pubic symphysis loading → reduced glute recruitment, may describe adaptations to chronic discomfort which did not reverse over a 20 minute post-fit trial, consistent with Bini (2020)'s findings that RPE responds faster than most motor-output variables to acute saddle adjustments.

The strongest sex×session finding was **perceptual**. A possible explanation is that an equal positional change relieves anatomical hotspots between sexes: male pudendal and ischial soft-tissue are unloaded onto the ischial tuberosities, whereas for females it could maintain or increase pubic-symphysis pressure, due to the broader pubic arch preventing ischial support at the same saddle width (Larsen et al., 2018; Lin et al., 2023). Pedal asymmetry supports this interpretation with females shifting towards right-side loading and males moving towards symmetry.

Regarding H2, a professional fit produces comparable saddle-pressure and postural changes in both sexes, but the psychological and motor-balance consequences of those changes are sex-specific. This claim is better evidenced and consistent with Dixon et al. (2017)'s suggestion that females require sex-specific equipment rather than scaled male defaults.

6.4 Neuromuscular dominance of the fit signal (H3)

Both random-forest classifiers weighted neuromuscular importance over metabolic, mechanical and subjective features. This is consistent with Chapman et al. (2009)'s claim that sEMG data carries more valuable positional adaption information. The female classifier weighted neuromuscular features more heavily than the male classifier (Table 6), supporting the key idea of this study that fit quality cannot be determined off kinematic data alone. The most important muscles in the female classifier (left hamstring, right glute) are those implicated in Potter et al. (2008)'s pelvic-tilt model, but those that are stronger in the male model (left shin, lower back, VO_2 slope) reflect a more mixed muscle recruitment strategy.

As kinematic features were not at sufficient completeness in the final feature matrix (Figure 32), the H3 contrast run here is neuromuscular vs (metabolic + mechanical), not the purely neuromuscular vs kinematic comparison initially planned.

6.5 Cross-modal coupling and the mechanical-to-metabolic lag (H4)

Twelve cross-modal Δ score correlations reached $|r_s| \geq 0.35$ (253 tested). Participants whose hamstring activation increased post-fit also tended to shift towards a more aerobic profile. This is because increased hamstring use through the downstroke will recruit a higher proportion of type 1 fibres (Rouffet and Hautier, 2008) and may shift the oxidative vs. glycolytic balance. ΔVE tracks ΔRPE at 19 min, while neither track Δbike-power, confirming that the **subjective** cost of the fit was driven by ventilation rather than mechanical load, mirroring the H1 interpretation that the fit moved participants into a ventilation heavy operating point, supported by the fact that VO_2/kg rose more for females who also reported a higher RPE post-fit.

The correlation of cadence against heart rate showed a bimodal distribution with modes at 0 s and 30 s (the search boundary), with a median peak lag of 18 s. As 46% of sessions saturated at 30 s, a wider window may have pushed the median higher. Because of this, the sample-level fusion, which assumes no lag, would have attributed

metabolic responses to the incorrect biomechanical state in over 80% of trials.

6.6 Methodological contribution

This study offers three contributions that may be transferable to other multi-modal sports-science research: 1. The data quality pipeline enforces feature-level fusion on the basis of a measured lag distribution, addressing the registration problem highlighted by Lahat et al. (2015); Millour et al. (2023) directly rather than through estimated alignment. 2. The per-sex classification strategy gives better clarity of feature importance per sex rather than being dominated by a specific group (Garnica-Caparrós and Memmert, 2021). 3. The use of several correction techniques in parallel (raw, Benjamini-Hochberg FDR, Bonferroni) allows discrimination between stable effects (VCO_2, saddle total force, COP_y shift) and exploratory effects (most within-sex paired tests).

6.7 Practical implications

The most actionable finding for professional fitters is that a relatively short gross road positioning fit reliably redistributed load from the saddle and onto the handlebars for both sexes, shift the CoP posteriorly by ~5 mm and allowed for much more consistent VO_2 slopes. These positional and pressure differences are usual indicators of a successful fit and do not require laboratory equipment to reproduce, a load sensing handlebar and saddle would suffice. For females the data suggests that the fit was just as successful as it was for men but questions remain over psychophysical and balance consequences of the new position. For industry, our data reinforces Dixon et al. (2017)'s claim that fit protocols and equipment sizing should not assume that male derived equations and benchmarks generalise.

6.8 Future directions

Four lines of work naturally follow: 1. A completed Mo-cap cohort such that the full neuromuscular vs kinematic test (H3) can be run.

2. The reframed H2 finding on RPE responses should be replicated using within-session comfort ratings collected at the same times as RPE. This would help determine if the post-fit RPE elevation in females was due to habituation effects or saddle interface limitations.

3. Positive ΔVO_2/kg-Δhamstring EMG coupling suggests that targeted hamstring recruitment cues during fitting could be beneficial for female cyclists. A controlled trial changing saddle setback would test this.

4. This study was based around power output and comfort; to further increase realism and fit profiles, the motion capture systems could be used to calculate frontal area and estimate drag, giving a better estimate of speed in a competitive setting.

6.9 Limitations

6.9.1 Session Order. For all but 4 participants session 2 preceded session 3, so the pre/post-fit order was not counterbalanced. This was a design choice to mirror real world order, balance the limited availability with our bike fitter and also to mitigate the risk of participants coming for the fit and not returning for a following session. The fixed order may have affected results due to fatigue or familiarisation with the static bike. Future studies should counterbalance the order of sessions to avoid any confounds.

6.9.2 Power Estimation and Erg Mode. FTP was estimated through a ramp test with an increase of 25W/min. The inclusion of this session was chosen due to the diversity of cycling experience in participants, meaning some would have no prior knowledge of threshold ranges for the 20 minute sessions, which was needed to ensure participants were working at similar relative power. However, the ramp test systematically overestimated FTP for less experienced cyclists. As the test lasts longer the more watts are needed, those who got a comparatively lower score would have had a shorter test, reflecting anaerobic ceiling rather than sustainable aerobic load. This meant that when some participants attempted a 20 minute session at their estimated FTP (in erg mode) they entered a feedback loop where reduced cadence led to increased resistance, which accelerated fatigue. The mitigation protocol for this ensured data continuity but introduced an extra variable. Participants that had power reduced may have completed their trial at a lower relative intensity, potentially impacting physiological stress in the EMG, metabolic and NIRS data. Session 3 was conducted at the lowest wattage from session 2, meaning that comparisons for affected participants should be interpreted with caution. Future work should consider a more thorough approach to determine threshold zones, especially if working with novices, potentially incorporating both a ramp test and a verification trial at the calculated threshold. Several participants reported that cycling on a static bike felt unfamiliar and that erg mode may have changed the way they would normally approach a session like that. Concerns like these are inherent to lab-based cycling research, and may affect generalisability of findings onto road/track conditions.

6.9.3 Hardware Constraints. The insole pressure sensors only had three available sizes (EU 41, 44, 47), meaning participants outside of these ranges either couldn't use them or would have potential noise due to cramping of sensors. Partway through session 3 these pressure boards began recording maximum values, likely due to heavy use that had not been thoroughly tested. Foot pressure data affected by this was excluded from analysis.

Both saddle and handlebars could not be exchanged during the fitting due to the integrated strain gauges and pressure sensors. Variables such as saddle selection, saddle angle, bar width and hood position would be addressed in a complete fitting. One participant could not achieve a low enough saddle position due to the hardware's adjustment range.

The left glute sEMG and IMU data streams were lost across data collection due to a software integration failure during recording. Therefore, claims around gluteal activation in this paper lie on data for the right-side alone.

Skinfold thickness was not measured at each NIRS site. Feldmann et al. (2019) found that SmO_2 reading reliability degrades above 15mm adipose tissue thickness, and Belzunce et al. (2023) found that females have greater subcutaneous fat around the glutes. Without site-specific skinfold data we cannot determine if SmO_2 signals could have been affected, future studies should record this to enable post-hoc quality assessment.

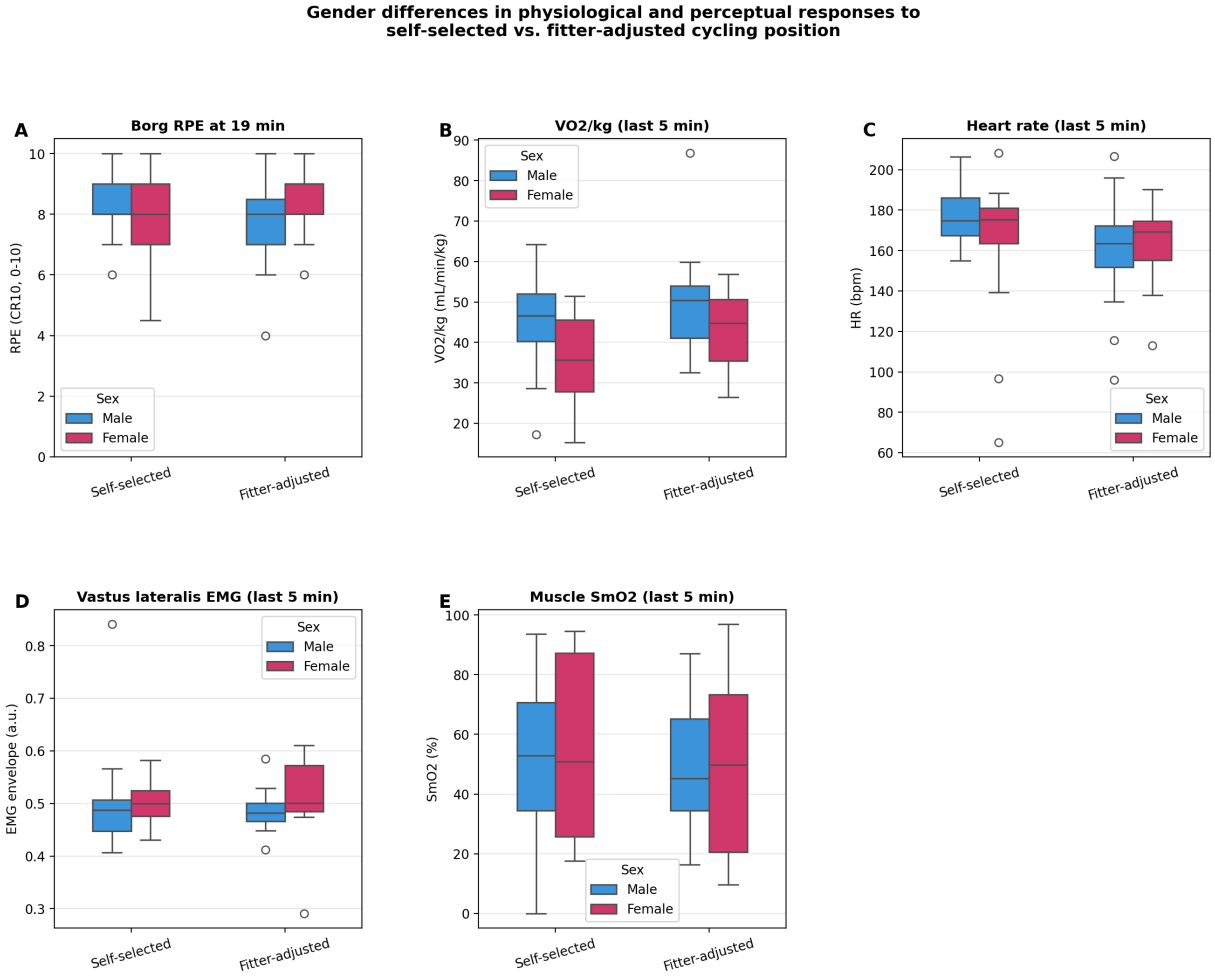


Fig. 5. Summary integrating the four hypothesis outcomes with the key effect sizes and the sex-specific RPE interaction.

Body hair was not controlled as a requirement. Participants were advised that sensor sites should ideally be shaved but this was not enforced. Particularly hairy skin can introduce noise in EMG sensors as well as risking reducing the adhesiveness of tape used to apply sensors.

6.9.4 Metabolic Measurements. Resting metabolic rate was not measured as it would have required an additional fasted lab visit as well as stricter pre-session dietary controls which were not feasible. This meant only gross efficiency (work output / metabolic expenditure) was calculated instead of net efficiency (work output / (total energy expenditure - resting metabolic rate)), which would have provided a more precise measure by accounting for baseline costs. This is relevant to sex-stratified analysis as resting metabolic rate is systematically different between sexes even after normalising for body weight, this means that observed sex differences may reflect baseline differences rather than just fitting-induced changes. Comfort was not recorded as an additional subjective measure. Bini (2020) found that comfort responds more sensitively than RPE when changing saddle height, so this would potentially allow for another dimension of analysis. This decision was made as sessions were separated by several weeks, making comparative comfort judgements unreliable. However, a comfort rating assessment within sessions at fixed times would be recommended for future research.

6.9.5 Sample Characteristics. 51 participants were university students aged 18-24 (with one participant aged 33), highlighting a narrow spread of age demographic. The experience classification (defined as cycling for more than 2 hours per week) does not distinguish between aerobic fitness and cycling-specific motor skill. This led to placing individuals into the inexperienced group even though they had a very good aerobic fitness, mostly those from the rowing club. A better definition incorporating competitive level and years of regular cycling, with more groups would allow for better group-based analysis. All fittings were performed by a single IBFI level 4 fitter. This ensured consistency across participants, but also means that results will reflect a single professional's methodology

and may not be generalisable to other fitters in the industry. Multiple fitters would be required to draw conclusions on the industry as a whole. Pre-session activity levels were not strictly controlled past instructing participants to abstain from caffeine, alcohol and vigorous exercise in the 24 hours preceding a session. Compliance with this varied, with one notable factor being the Bath Half marathon, which multiple participants stated impacted their fatigue. Similarly, resting heart rate was recorded mid-day, after participants had been active (including some cycling to campus). This compounded with a possible white-coat effect likely caused elevated estimates for resting heart rate (Pickering et al., 2002).

6.9.6 Analytical Scope. Time and sample constraints limited some analytical approaches discussed in the literature review. Inverse dynamics modelling with OpenSim would have allowed joint movement and muscle force estimation. Supervised ML classification models were not pursued. 36 complete participants in a 2×2 design (condition × sex) would be insufficient for reliable training and validation of classification models, meaning feature importance analysis would likely be underpowered and at high risk of over fitting. Both of these methods would be viable for larger cohorts.

7 Conclusion

This study explored whether a professional bike fit produced significant changes in biomechanical and physiological efficiency, whether those changes differed between sexes and whether neuromuscular signals carried more information about fit quality than kinematic or metabolic signals. To tackle these questions synchronised multimodal data was collected from 51 cyclists before and after a standardised IBFI level-4 fit and analysed through a feature-level fusion pipeline.

Four findings emerged from the study: 1. The fit produced a small but consistent ventilation-led efficiency signature (H1). VCO_2 and left-calf sEMG survived FDR correction at $q < .05$, with $VO_2\,kg^{-1}$, tidal volume, energy expenditure, heart rate and right-calf SmO_2 all trending in the same direction. 2. The prediction that females would show larger saddle pressure and gluteal activation changes (H2) was not supported. Total saddle force, posterior CoP shift and handlebar loading changed by comparable magnitudes in both sexes. The clearest sex interaction was instead perceptual, end-trial RPE fell by 0.58 points in males but rose by 0.5 points in females. 3. Sex-specific random forest classifiers weighted neuromuscular features above metabolic, mechanical and subjective features (H3), with 62.5% and 55.1% of total importance for females and males respectively. 4. Twelve Δ-score correlations achieved $|r_s| \geq 0.35$, notably $\Delta VO_2\,kg^{-1}$ coupled positively to Δhamstring EMG and negatively to ΔRQ, and ΔVE tracked ΔRPE at 19 min while neither tracked bike power, indicating that the subjective cost of the fit was driven by ventilation rather than by mechanical load.

These findings suggest that current fitting practice (which is largely derived from male-calibrated formulae) only captures part of the female-specific response. Handlebar and saddle adjustments translate between sexes but perceptual and neuromuscular costs diverge, with female cyclists relying on higher gluteal and hamstring activation to achieve similar metabolic profiles. Our findings demonstrated that multi-modal, lag aware analysis can detect positional responses that kinematics alone may miss and provide quantitative support for the view that females would benefit from sex-specific protocols rather than scaled male defaults.
Word Count = 10,266

8 Contributions

This study formed part of the Impact Lab Bikefit project. The author (Matthew Pearson) was responsible for: (i) leading recruitment, scheduling and running of all 138 lab sessions, training fellow researchers; (ii) integration testing of the sensor stack across pilot sessions and designing the pre-session protocol; (iii) the data pipeline, from raw multi-stream parsing through feature-level fusion to the inferential and exploratory analyses reported in this paper; (iv) all hypothesis design, statistical analysis, figures, tables and writing.

9 Acknowledgments

The author would also like to thank the following: Hugo Hafner (co-researcher, final-year project student) attended roughly 90% of data collection session, running an independent project on the data gathered.
Tarini Sehgal (departmental intern) supported roughly 10% of data collection sessions and will conduct remaining sessions after our internal collection-cutoff, alongside Anca Salagean.
The Bikefit web platform, as well as IRIS motion capture, was developed by the Bath Impact lab software team (Mark Townsend, Max Ashton, Victor Idongesit, Trishan Dissanayake). Technical support and custom hardware including pressure sensors, strain gauges and tidal flow sensors were developed by the Lovelace lab team (Alvaro Favaratto Santos, Alex Deegan); see Appendix M. Bike fittings were provided by Tony Corke of Torke Cycling. Supervision was provided by Prof. Eamonn O'Neill and Dr. Crescent Jicol.

References

Allen, H. and Coggan, A. (2010), *Training and Racing with a Power Meter*, Velo Press Series, VeloPress.
URL: *https://books.google.co.uk/books?id=IYGHPgAACAAJ*

Atkinson, G., Peacock, O., St Clair Gibson, A. and Tucker, R. (2007), 'Distribution of power output during cycling', *Sports Medicine* **37**(8), 647–667.
URL: *https://doi.org/10.2165/00007256-200737080-00001*

Baran, C., Mitchell, G. C. and Hellstrom, W. J. G. (2014), 'Cycling-related sexual dysfunction in men and women: A review', *Sexual Medicine Reviews* **2**(3), 93–101.

Belzunce, M. A., Henckel, J., Di Laura, A., Horga, L. M. and Hart, A. J. (2023), 'Similarities and differences in skeletal muscle and body composition between sexes: an mri study of recreational cyclists', *BMJ Open Sport & Exercise Medicine* **9**, e001672.

Bing, F., Zhang, G., Wei, L. and Zhang, M. (2025), 'A machine learning approach for saddle height classification in cycling', *Frontiers in Sports and Active Living* **7**, 1607212.

Bini, R. R. (2020), 'Acute effects from changes in saddle height in perceived comfort during cycling', *International Journal of Sports Science & Coaching* **15**(3), 390–397.

Bini, R. R., Diefenthaeler, F. and Mota, C. B. (2010), 'Fatigue effects on the coordinative pattern during cycling: kinetics and kinematics evaluation', *Journal of Electromyography and Kinesiology* **20**(1), 102–107.

Bouillod, A., Oggiano, L., Soto-Romero, G., Brunet, E. and Grappe, F. (2016), Preliminary study: A new method to assess the effective frontal area of cyclists, *in* 'Proceedings of the 4th International Congress on Sport Sciences Research and Technology Support (IcSPORTS)', Porto, Portugal. HAL Id: hal-01385084.

Buchanan, T. S., Lloyd, D. G., Manal, K. and Besier, T. F. (2005), 'Estimation of muscle forces and joint moments using a forward-inverse dynamics model', *Medicine & Science in Sports & Exercise* **37**(11), 1911–1916.

Burt, P. (2022), *Bike fit 2nd edition: optimise your bike position for high performance and injury avoidance*, Bloomsbury publishing.

Carpes, F. P., Mota, C. B. and Faria, I. E. (2010), 'On the bilateral asymmetry during running and cycling – a review considering leg preference', *Physical Therapy in Sport* **11**(4), 136–142.
URL: *https://www.sciencedirect.com/science/article/pii/S1466853X10000490*

Ceseracciu, E., Sawacha, Z. and Cobelli, C. (2014), 'Comparison of markerless and marker-based motion capture technologies through simultaneous data collection during gait: proof of concept', *PloS one* **9**(3), e87640.

Challis, J. H. (2021), *Electromyography*, Springer International Publishing, Cham, pp. 69–80.
URL: *https://doi.org/10.1007/978-3-030-52256-8*$_5$

Chapman, A. R., Vicenzino, B., Blanch, P. and Hodges, P. W. (2008), 'Patterns of leg muscle recruitment vary between novice and highly trained cyclists', *Journal of Electromyography and Kinesiology* **18**(3), 359–371.

Chapman, A., Vicenzino, B., Blanch, P. and Hodges, P. (2009), 'Do differences in muscle recruitment between novice and elite cyclists reflect different movement patterns or less skilled muscle recruitment?', *Journal of Science and Medicine in Sport* **12**(1), 31–34.

Chung, S., Lim, J., Noh, K. J., Kim, G. and Jeong, H. (2019), 'Sensor data acquisition and multimodal sensor fusion for human activity recognition using deep learning', *Sensors* **19**(7).
URL: *https://www.mdpi.com/1424-8220/19/7/1716*

de Vey Mestdagh, K. (1998), 'Personal perspective: in search of an optimum cycling posture', *Applied Ergonomics* **29**(5), 325–334.
URL: *https://www.sciencedirect.com/science/article/pii/S000368709700080X*

Dettori, N. J. and Norvell, D. C. (2006), 'Non-traumatic bicycle injuries', *Sports Medicine* **36**(1), 7–18.

Dixon, M. A., Graham, J. A., Hartzell, A. C. and Forrest, K. (2017), 'Enhancing women's participation and advancement in competitive cycling', *Journal of Applied Sport Management* **9**(4).
URL: *https://voljournals.utk.edu/jasm/vol9/iss4/6*

D'Souza, S., Siebert, T. and Fohanno, V. (2024), 'A comparison of lower body gait kinematics and kinetics between theia3d markerless and marker-based models in healthy subjects and clinical patients', *Scientific Reports* **14**(1), 29154.

Encarnación-Martínez, A., Ferrer-Roca, V. and García-López, J. (2021), 'Influence of sex on current methods of adjusting saddle height in indoor cycling', *Journal of Strength and Conditioning Research* **35**(2), 519–526.

Ettema, G., Lorås, H. and Leirdal, S. (2009), 'The effects of cycling cadence on the phases of joint power, crank power, force and force effectiveness', *Journal of Electromyography and Kinesiology* **19**(2), e94–e101.
URL: *https://www.sciencedirect.com/science/article/pii/S1050641107001903*

Feldmann, A., Schmitz, R. and Erlacher, D. (2019), 'Near-infrared spectroscopy-derived muscle oxygen saturation on a 0% to 100% scale: reliability and validity of the moxy monitor', *Journal of Biomedical Optics* **24**(11), 115001.

Fintelman, D., Sterling, M., Hemida, H. and Li, F.-X. (2015), 'The effect of time trial cycling position on physiological and aerodynamic variables', *Journal of Sports Sciences* **33**(16), 1730–1737. PMID: 25658151.
URL: *https://doi.org/10.1080/02640414.2015.1009936*

Fonda, B., Sarabon, N. and Li, F.-X. (2014), 'Validity and reliability of different kinematics methods used for bike fitting', *Journal of Sports Sciences* **32**(10), 940–946. PMID: 24499342.
URL: *https://doi.org/10.1080/02640414.2013.868919*

Garnica-Caparrós, M. and Memmert, D. (2021), 'Understanding gender differences in professional european football through machine learning interpretability and match actions data', *Scientific Reports* **11**, 10805.

Harsted, S., Holsgaard-Larsen, A., Hestbæk, L., Boyle, E. and Lauridsen, H. H. (2019), 'Concurrent validity of lower extremity kinematics and jump characteristics captured in pre-school children by a markerless 3d motion capture system', *Chiropractic & Manual Therapies* **27**(1), 39.

Heil, D. (2001), 'Body mass scaling of projected frontal area in competitive cyclists', *European Journal of Applied Physiology* **85**(3), 358–366.

Hoffmann, R., Schwöbel, C., Kelkel, D. and Leyendecker, S. (2024), 'Gender differences in cycling motions: On objective functions for urban cycling', *Proceedings in Applied Mathematics and Mechanics* **24**(1), e202300202.
URL: *https://onlinelibrary.wiley.com/doi/abs/10.1002/pamm.202300202*

Horsak, B., Eichmann, A., Lauer, K., Prock, K., Krondorfer, P., Siragy, T. and Dumphart, B. (2023), 'Concurrent validity of smartphone-based markerless motion capturing to quantify lower-limb joint kinematics in healthy and pathological gait', *Journal of Biomechanics* **159**, 111801.
URL: *https://www.sciencedirect.com/science/article/pii/S002192902300372X*

Husband, S. P., Wainwright, B., Wilson, F., Crump, D., Mockler, D., Carragher, P., Nugent, F. and Simms, C. K. (2024), 'Cycling position optimisation – a systematic review of the impact of positional changes on biomechanical and physiological factors in cycling', *Journal of Sports Sciences* **42**(15), 1477–1490. PMID: 39285616.
URL: *https://doi.org/10.1080/02640414.2024.2394752*

Jones, A. M., Grassi, B., Christensen, P. M., Krustrup, P., Bangsbo, J. and Poole, D. C. (2011), 'Slow component of $\dot{V}o_2$ kinetics: Mechanistic bases and practical applications', *Medicine & Science in Sports & Exercise* **43**(11), 2046–2062.

Katmah, R., Shehhi, A. A., Jelinek, H. F., Hulleck, A. A. and Khalaf, K. (2023), 'A systematic review of gait analysis in the context of multimodal sensing fusion and ai', *IEEE Transactions on Neural Systems and Rehabilitation Engineering* **31**, 4189–4202.

Kearney, J., Greaves, H., Robinson, M. A., Barton, G. J., O'Brien, T. D., Pinzone, O., Wright, D. M., Gibbon, K. and Foster, R. J. (2025), 'Comparison of theia3d and the conventional gait model in typically developing children and adults in a clinical gait laboratory', *Journal of Biomechanics* **193**, 112995.
URL: *https://www.sciencedirect.com/science/article/pii/S002192902500507X*

Koopman, B., Grootenboer, H. J. and de Jongh, H. J. (1995), 'An inverse dynamics model for the analysis, reconstruction and prediction of bipedal walking', *Journal of Biomechanics* **28**(11), 1369–1376.
URL: *https://www.sciencedirect.com/science/article/pii/0021929094001857*

Korzeniewski, B. and Zoladz, J. A. (2015), 'Possible mechanisms underlying slow component of vo2 on-kinetics in skeletal muscle', *Journal of Applied Physiology* **118**(10), 1240–1249. PMID: 25767031.
URL: *https://doi.org/10.1152/japplphysiol.00027.2015*

Kotler, D. (2023), 'Training and injury considerations in female-identifying cyclists', *Journal of Women's Sports Medicine* **3**(2), 11–24.
URL: *https://www.jwomenssportsmed.org/index.php/jwsm/article/view/45*

Lahat, D., Adali, T. and Jutten, C. (2015), 'Multimodal data fusion: An overview of methods, challenges, and prospects', *Proceedings of the IEEE* **103**(9), 1449–1477.

Larsen, A. S., Larsen, F. G., Sørensen, F. F., Hedegaard, M., Støttrup, N., Hansen, E. A. and Madeleine, P. (2018), 'The effect of saddle nose width and cutout on saddle pressure distribution and perceived discomfort in women during ergometer cycling', *Applied Ergonomics* **70**, 175–181.
URL: *https://www.sciencedirect.com/science/article/pii/S0003687018300632*

Li, J., Wang, Q., Zhang, Y., Zhang, L., Dong, G., Ma, G., Peng, S., Wang, B., Wang, J., Zhou, J. and Bao, D. (2025), 'Effects of crank length on cycling efficiency, sprint performance, and perceived fatigue in high-level amateur road cyclists', *Journal of Exercise Science Fitness* **23**(3), 175–180.
URL: *https://www.sciencedirect.com/science/article/pii/S1728869X25000280*

Lin, Z.-J., Wang, H.-H. and Chen, C.-H. (2023), 'The effect of bicycle saddle widths on saddle pressure in female cyclists', *Journal of Sports Science & Medicine* **22**(3), 425.

Liparoti, M., Troisi Lopez, E. and Agosti, V. (2020), 'Motion capture system: a useful tool to study cyclist's posture', *Journal of Physical Education and Sport* **20**(Supplement issue 4), 2364–2367.

Lucía, A., Hoyos, J. and Chicharro, J. L. (2000), 'The slow component of vo2 in professional cyclists', *British Journal of Sports Medicine* **34**(5), 367–374.
URL: *https://bjsm.bmj.com/content/34/5/367*

Malizia, F. and Blocken, B. (2021), 'Cyclist aerodynamics through time: Better, faster, stronger', *Journal of Wind Engineering and Industrial Aerodynamics* **214**, 104673.
URL: *https://www.sciencedirect.com/science/article/pii/S0167610521001574*

Martin, J. C. and Brown, N. A. (2009), 'Joint-specific power production and fatigue during maximal cycling', *Journal of Biomechanics* **42**(4), 474–479.
URL: *https://www.sciencedirect.com/science/article/pii/S0021929008006015*

Martin, J. C. and Nichols, J. A. (2018), 'Simulated work loops predict maximal human cycling power', *Journal of Experimental Biology* **221**(13), jeb180109.

Millour, G., Torres Velásquez, A. and Domingue, F. (2023), 'A literature overview of modern biomechanical-based technologies for bike-fitting professionals and coaches', *International Journal of Sports Science & Coaching* **18**(1), 292–303.

Peeters, T., Garimella, R., Francken, E., Henderieckx, S., van Nunen, L. and Verwulgen, S. (2021), The correlation between frontal area and joint angles during cycling, *in* D. N. Cassenti, S. Scataglini, S. L. Rajulu and J. L. Wright, eds, 'Advances in Simulation and Digital Human Modeling', Springer International Publishing, Cham, pp. 251–258.

Pickering, T. G., Gerin, W. and Schwartz, A. R. (2002), 'What is the white-coat effect and how should it be measured?', *Blood Pressure Monitoring* **7**(6), 293–300.

Potter, J. J., Sauer, J. L., Weisshaar, C. L., Thelen, D. G. and Ploeg, H.-L. (2008), 'Gender differences in bicycle saddle pressure distribution during seated cycling', *Medicine & Science in Sports & Exercise* **40**(6), 1126–1134.

Pottinger, M. V. (2018), Inverse dynamic analysis of acl reconstructed knee joint biomechanics during gait and cycling using opensim, Master's thesis, California Polytechnic State University.

Priego Quesada, J. I., Kerr, Z. Y., Bertucci, W. M. and Carpes, F. P. (2019), 'The association of bike fitting with injury, comfort, and pain during cycling: An international retrospective survey', *European Journal of Sport Science* **19**(6), 842–849.
URL: *https://onlinelibrary.wiley.com/doi/abs/10.1080/17461391.2018.1556738*

Procházka, A., Vaseghi, S., Charvátová, H., Ťupa, O. and Vyšata, O. (2017), 'Cycling segments multimodal analysis and classification using neural networks', *Applied Sciences* **7**(6), 581.

Rouffet, D. M. and Hautier, C. A. (2008), 'Emg normalization to study muscle activation in cycling', *Journal of Electromyography and Kinesiology* **18**(5), 866–878.

Torres-Davis, R. (2026), '"We've got loads of amazing technology now, but fewer size options" – whatever happened to women-specific sizes?', Cycling Weekly. Originally published in print 5 March 2026. Accessed 21 April 2026.
URL: *https://www.cyclingweekly.com/products/weve-got-loads-of-amazing-technology-now-but-fewer-size-options-whatever-happened-to-women-specific-sizes*

Vicari, D. S. S., Patti, A., Giustino, V., Figlioli, F., Zangla, D., Maksimovic, N., Drid, P., Palma, A. and Bianco, A. (2025), 'Saddle pressures distribution at different pedaling intensities in young off-road cyclists: focus on sex', *Annals of Medicine* **57**(1), 2495764. PMID: 40298622.
URL: *https://doi.org/10.1080/07853890.2025.2495764*

Wangerin, M., Schmitt, S., Stapelfeldt, B. and Gollhofer, A. (2007), Inverse dynamics in cycling performance, *in* T. M. Buzug, D. Holz, J. Bongartz, M. Kohl-Bareis, U. Hartmann and S. Weber, eds, 'Advances in Medical Engineering', Springer Berlin Heidelberg, Berlin, Heidelberg, pp. 329–334.

Wren, T. A., Isakov, P. and Rethlefsen, S. A. (2023), 'Comparison of kinematics between theia markerless and conventional marker-based gait analysis in clinical patients', *Gait Posture* **104**, 9–14.
URL: *https://www.sciencedirect.com/science/article/pii/S0966636223001443*

Wu, Y., Ma, Z., Zhao, H., Li, Y. and Sun, Y. (2020), 'Achieve personalized exercise intensity through an intelligent system and

cycling equipment: A machine learning approach', *Applied Sciences* **10**(21).
URL: *https://www.mdpi.com/2076-3417/10/21/7688*

Zakaria, D., Kramer, J. F. and Harburn, K. L. (1996), 'Reliability of non-normalized and normalized integrated emg during maximal isometric contractions in females', *Journal of Electromyography and Kinesiology* **6**(2), 129–135.
URL: *https://www.sciencedirect.com/science/article/pii/1050641195000259*

A Participant recruitment

Recruitment and participant management was lead by myself. I deigned the recruitment poster (below) and messaged university groups including cycling, triathlon and rowing (as a means of getting lesser experienced cyclists) and sending information sheets to everyone who expressed interest. I then ensured consent forms were filled out by every participant and began to schedule sessions. Testing took place over a period of 8 weeks, coinciding with the beginning of semester 2 until the Easter break. I had the task of noting all researcher's availability and then scheduling in all 138 sessions that were completed before our data collection cut-off.

B Sensor Locations

Table 8. Comprehensive Mapping of Heterogeneous Sensor Channels

Channel ID	Anatomical Target / Muscle
EMG 1 / 2	L/R Vastus Lateralis (Outer Quad)
EMG 3 / 4	L/R Gluteus Maximus
EMG 5 / 6	L/R Biceps Femoris (Hamstring)
EMG 7 / 8	L/R Medial Gastrocnemius (Calf)
EMG 9 / 10	L/R Latissimus Dorsi (Lats)
EMG 11 / 12	L/R Rectus Femoris (Front Quad)
EMG 13 / 14	L/R Tibialis Anterior (Shin)
EMG 15	R Erector Spinae (Lower Back)
EMG 16	L Deltoid (Shoulder)
NIRS 1 / 2	L/R Vastus Lateralis
NIRS 3 / 4	L/R Gluteus Maximus
NIRS 5 / 6	L/R Biceps Femoris
NIRS 7 / 8	L/R Medial Gastrocnemius
Force/Strain	Handlebars, Saddle, Footbeds
Kinematics	Full-body Markerless Mesh (17-seg)
Metabolic	Breath-by-breath Gas Analysis (VO_2)

C Fitting Protocol

The following details the fitting performed by Tony Corke:

Road gross positioning. No saddle change or angle adjustment, no inner shoe adjustment, no bar width or hood adjustment In our fitting we assessed cleat position (fore/aft) saddle height, saddle setback, reach to bars, bar height, weight distribution and crank length for range of movement. Body weight distribution. Feel of mass through contact points with the goal of trying to minimise weight through the hands without sacrificing ease of pedalling or power production.



Fig. 6. Recruitment poster

D Data collection hours

Data Collection was an extremely time consuming process for this project. We allowed: 1 hour for lab session 1, 90 minutes for lab session 2, 120 minutes for lab session 3.

Allowing for a setup time as well at an estimate of 30 minutes a day (for things such as COSMED warmup), 6 days a week, for 8 weeks. For the completed sessions this totals to 13410 minutes, or 223.5 hours of testing. I was not present for every session due to illness but completed roughly 200 hours of data collection. I also trained a researcher on our protocols so they could take over testing once our data collection deadline has passed. Including familiarisation with hard/software, participant management/scheduling, experimental planning and team meetings, over 250 hours was spent on data collection and its processes alone.

E Github repository for the data pipeline

The feature-fusion pipeline can be found at the following repository: https://github.com/Matthew8747/Bikefit-Data-Pipeline All raw data

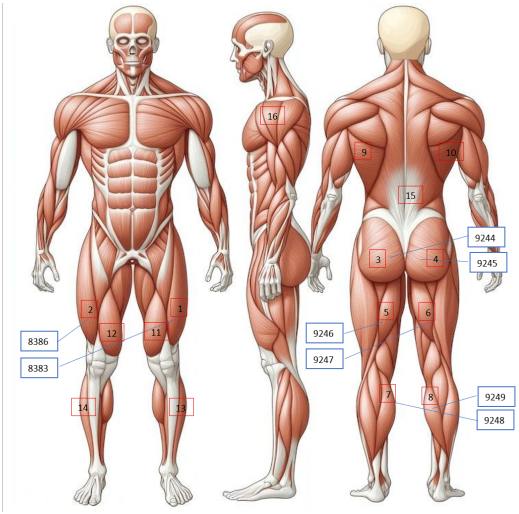


Fig. 7. Sensor Locations for Trigno (red box) and Moxy (blue box) sensors.

is not included due to file sizes. There is a sample of the Bikefit web platform data download.

F Camera Setup

This diagram shows how the motion capture cameras were positioned. The larger cameras represent markerless Qualysis cameras and the smaller ones are 1080p webcams used to record IRIS (the inbuilt university motion capture system being tested).

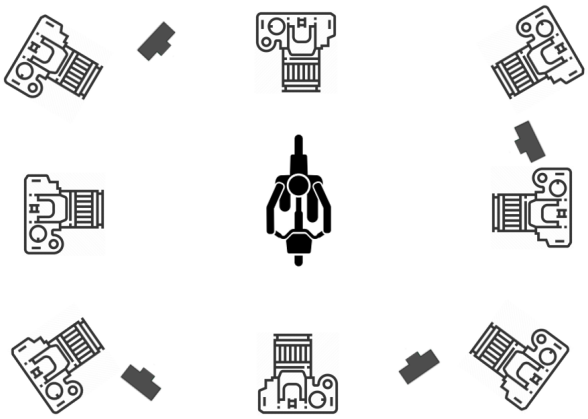


Fig. 8. Motion capture camera setup

G Inverse Dynamics Literature Review

The following was an extract from the literature review covering inverse dynamics. This was excluded from the main report as it was not pursued during the study

Inverse dynamics are needed to evaluate joint-level efficiency, calculating joint moments and powers from kinematic and force data. Pottinger (2018) demonstrated a full cycling analysis pipeline using OpenSim. Martin and Brown (2009) showed that hip and knee joints display distinct fatigue profiles during maximal cycling, suggesting joint-specific metrics would be preferable over aggregate efficiency. Martin and Nichols (2018) found bi-articular muscles often act as energy transfer systems as opposed to net power producers (bicep femoris long head contributed 150W to hip joint power, but 12W of metabolic output), highlighting importance of joint-level analysis.

Standard inverse dynamics faces the redundancy problem that net forces could have been formed from any number of individual muscle combinations. Buchanan et al. (2005) established a forward-inverse dynamics approach, using EMG as inputs to resolve individual muscle forces, which allows for the calculation of co-contraction cost. Koopman et al. (1995) showed that constraints such as fixing feet to pedals allows unmeasured variables to be reconstructed, a principle that would also help noisy markerless tracking data.

H Additional Graphs and Figures

The following pages collect all supporting figures and statistical tables produced by the analysis pipeline. Figures are grouped by modality / hypothesis. Where a figure exceeds the page height the layout has been rotated to landscape or given a dedicated float page.

H.1 Sample Characteristics and Data Integrity

Table 9. Participant demographics, stratified by sex. Values are mean ± SD unless stated. p-values from Mann-Whitney U tests on the raw distributions; d is Cohen's d for independent samples (positive values favour males).

Variable	Female (n = 24)	Male (n = 27)	d	p
Age (yr)	20.7 ± 3.1	20.2 ± 1.6	−0.26	0.92
Height (cm)	167.3 ± 7.5	182.3 ± 7.9	−1.94	<.001
Weight (kg)	60.8 ± 11.8	77.1 ± 13.0	−1.25	<.001
Inside leg (cm)	77.7 ± 4.8	82.4 ± 5.6	−0.90	0.003
FTP (W)	178.2 ± 52.7	257.7 ± 54.0	−1.47	<.001
Relative power (W kg^{-1})	3.01 ± 0.63	3.43 ± 0.70	−0.63	0.046
Cycling (h wk^{-1})	7.3 ± 18.3	3.5 ± 3.7	+0.33	0.87

Table 10. Per-session completeness of the six core modality streams. Cells report count (of 87 trials across 51 participants) satisfying the duration, HR-stability, power-stability and sensor-channel checks described in Section 4.1

Modality	S2 (self-fitted)	S3 (fitter-adjusted)
Demographics / RPE	51	36
Bike (power / cadence / HR)	51	36
sEMG (16 channels, 1259 Hz)	50	35
Moxy NIRS (8 channels)	46	34
COSMED (breath-by-breath)	50	36
Insole pressure	21	15
Mo-cap (Theia3D)	13	~6 (processing ongoing)

- Matthew Pearson

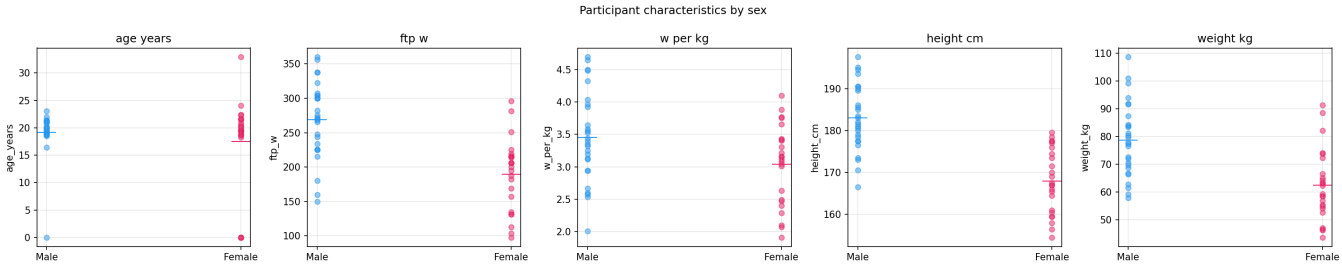


Fig. 9. Cohort demographic overview: age, height, weight, FTP, inseam and arm-length distributions stratified by sex ($n = 51$).

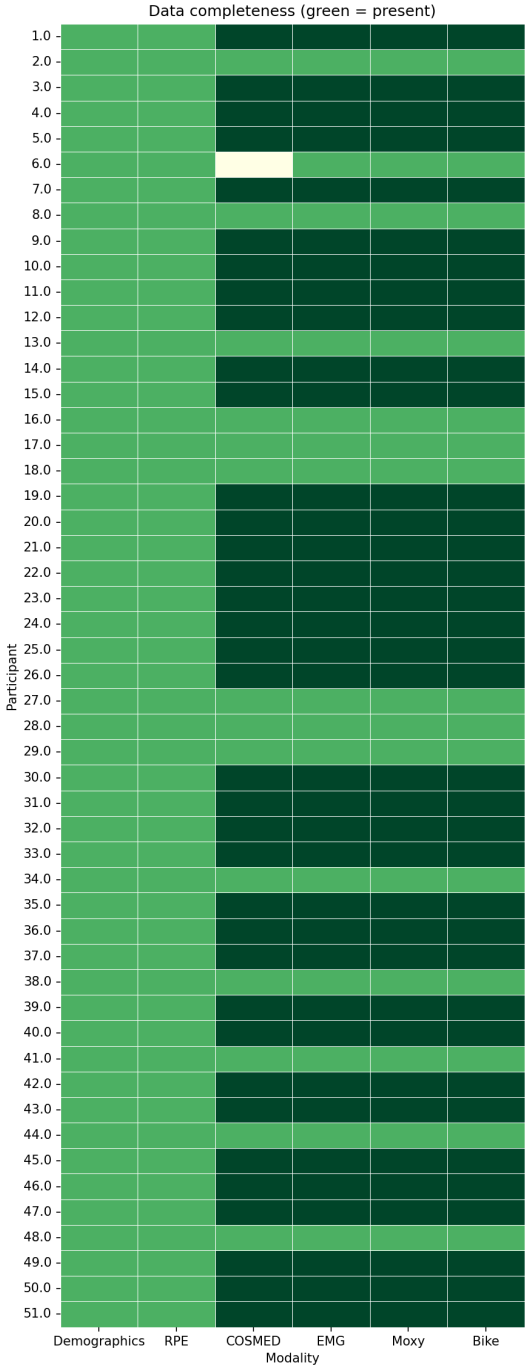


Fig. 10. Per-participant data completeness across the five main modalities. Dark green = both S2 and S3 present; light green = S2 only; pale = missing. 36 of 51 participants completed both sessions across all core modalities.

- Matthew Pearson

H.2 Subjective Exertion (RPE)

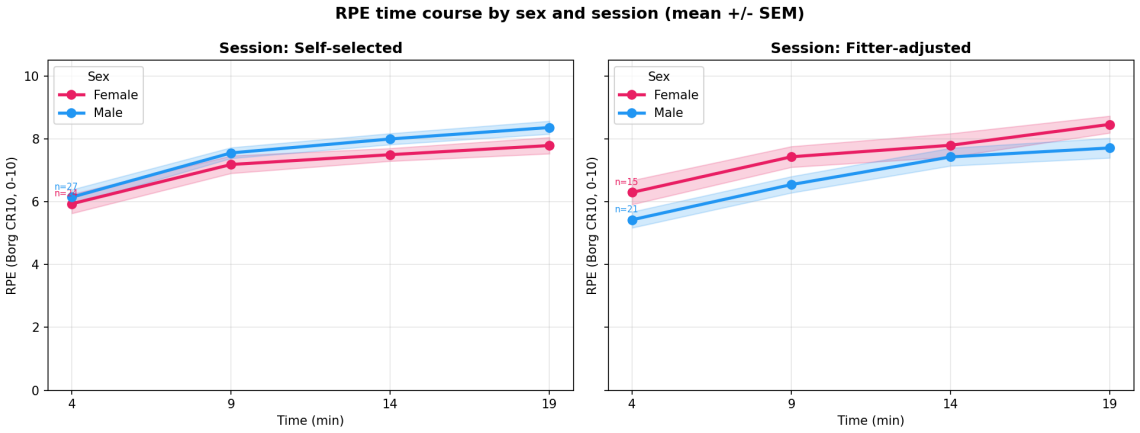


Fig. 11. Individual participant RPE time-courses (spaghetti plot) colour-coded by sex, both sessions superimposed.

Table 11. Bootstrap 95% confidence intervals ($n = 2000$ resamples) for key sex-stratified Δ-scores (S3−S2) and the male−female difference-of-deltas. Source: `bootstrap_cis.csv`.

Variable	Group	Mean Δ	95% CI lo	95% CI hi
RPE (19 min)	Male	−0.575	−1.075	−0.100
RPE (19 min)	Female	+0.500	−0.036	+1.000
RPE (19 min)	Male−Female	−1.075	−1.786	−0.343
VO_2/kg	Male−Female	−2.315	−9.631	+4.713
SmO_2 (right glute)	Male−Female	+7.395	−8.826	+24.593

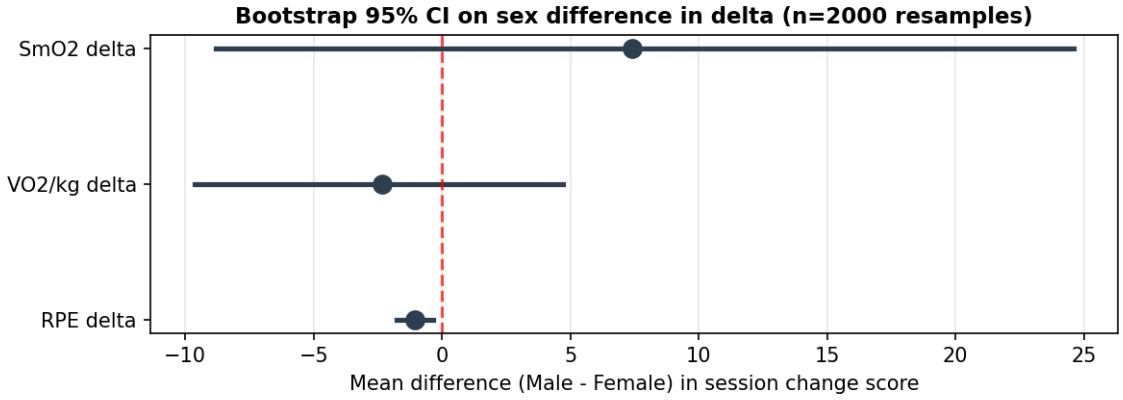


Fig. 12. Bootstrap 95% CIs for the sex-stratified Δ-scores tabulated in Table 11. Intervals that exclude zero indicate statistically stable differences at the 5% level.

H.3 Metabolic and Muscle Oxygenation

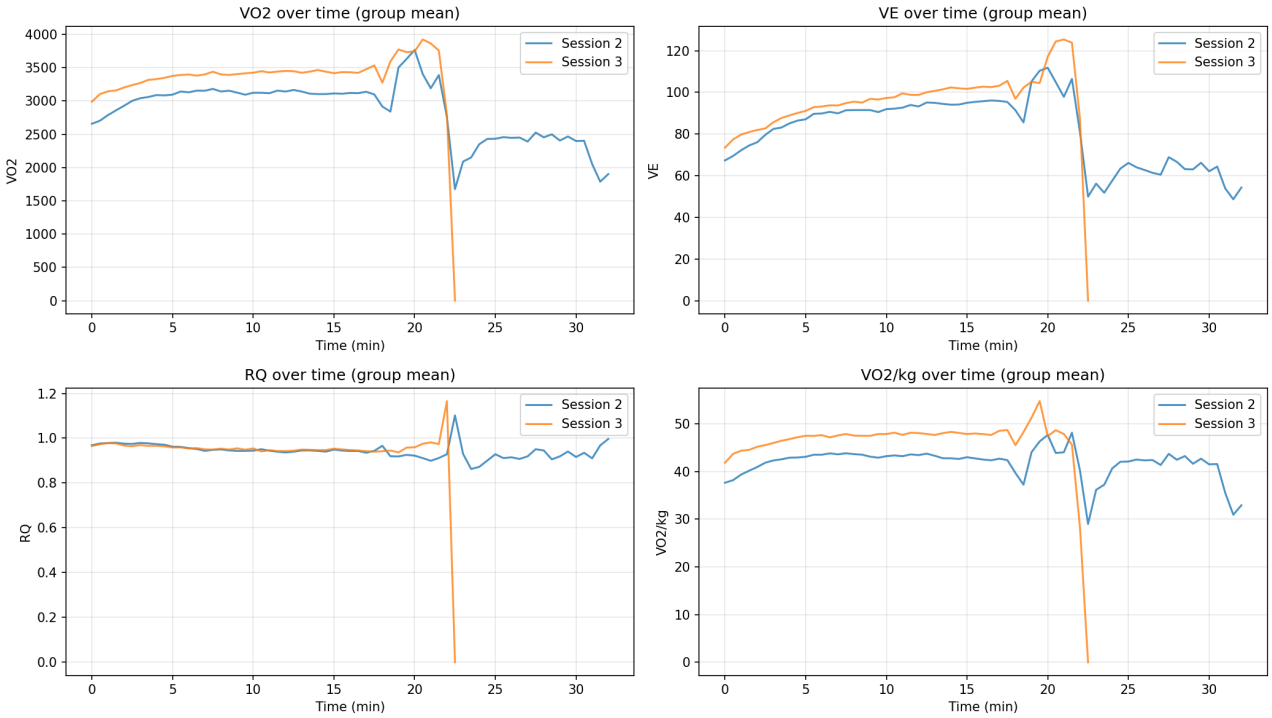
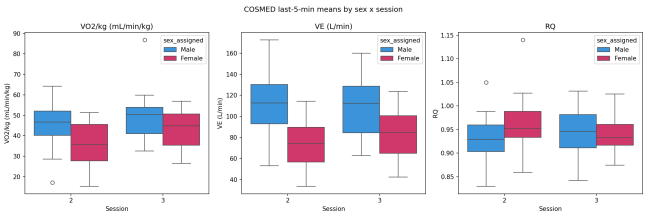
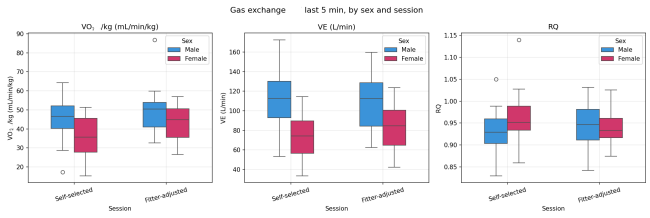


Fig. 13. COSMED breath-by-breath data: cohort summary of VO_2, VE, V_T, Rf, RQ and VCO_2 distributions by session.



(a) Summary cohort distributions.



(b) Sex-stratified last-5 min gas exchange.

Fig. 14. Metabolic summary from COSMED.

- Matthew Pearson

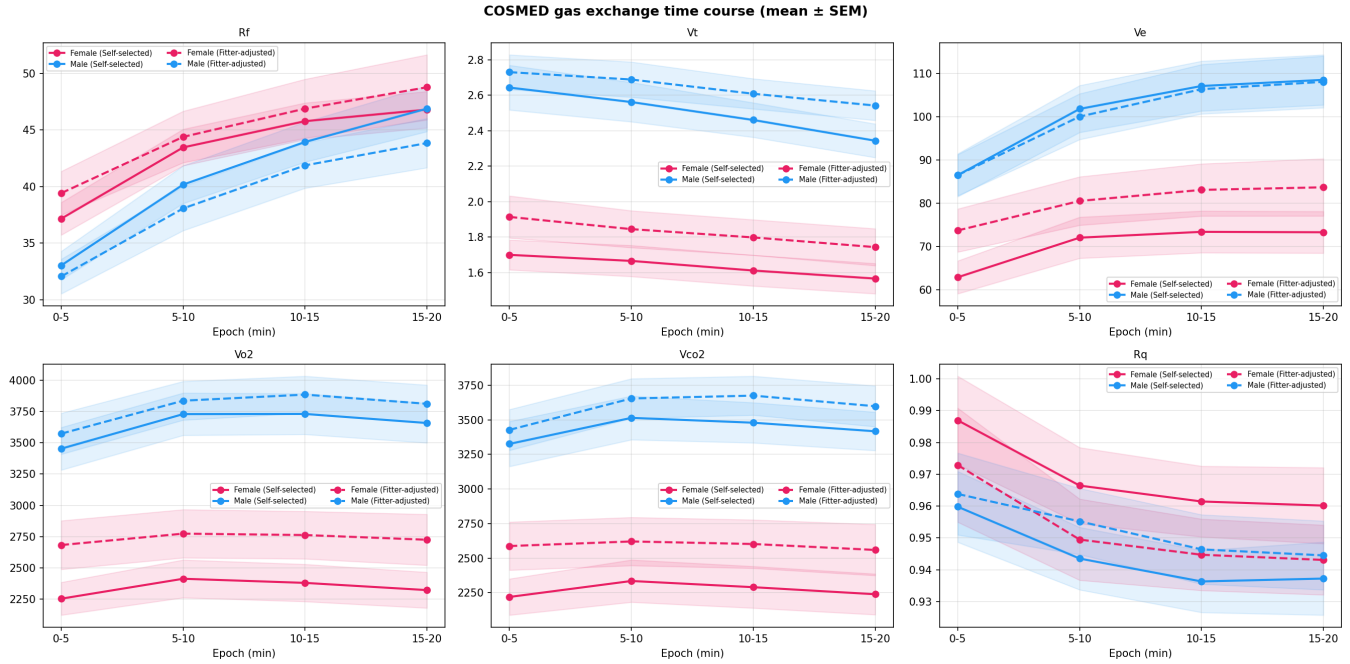
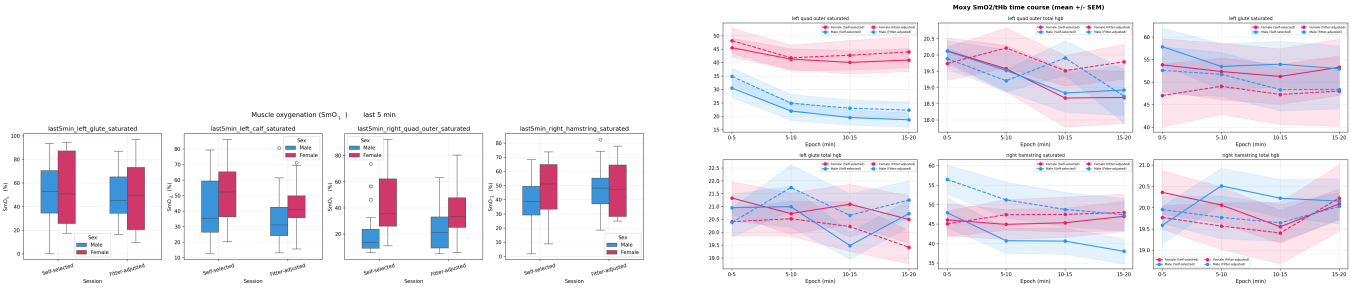


Fig. 15. Mean ± SEM time-course (0-5, 5-10, 10-15, 15-20 min epochs) for respiratory frequency (Rf), tidal volume (V_T), minute ventilation (VE), VO_2, VCO_2 and RQ, stratified by sex and session. Solid = self-fitted (S2), dashed = fitter-adjusted (S3).



(a) Muscle oxygenation (SmO_2) by sex and session.

(b) SmO_2 time-course across the 20-minute trial.

Fig. 16. Near-infrared spectroscopy (Moxy) muscle oxygen saturation. Right calf SmO_2 dropped 7.4% post-fit at cohort level ($d_z = -0.37$, $p_{FDR} = 0.10$).

H.4 Kinematics (Theia3D Markerless Mo-cap)

- Matthew Pearson

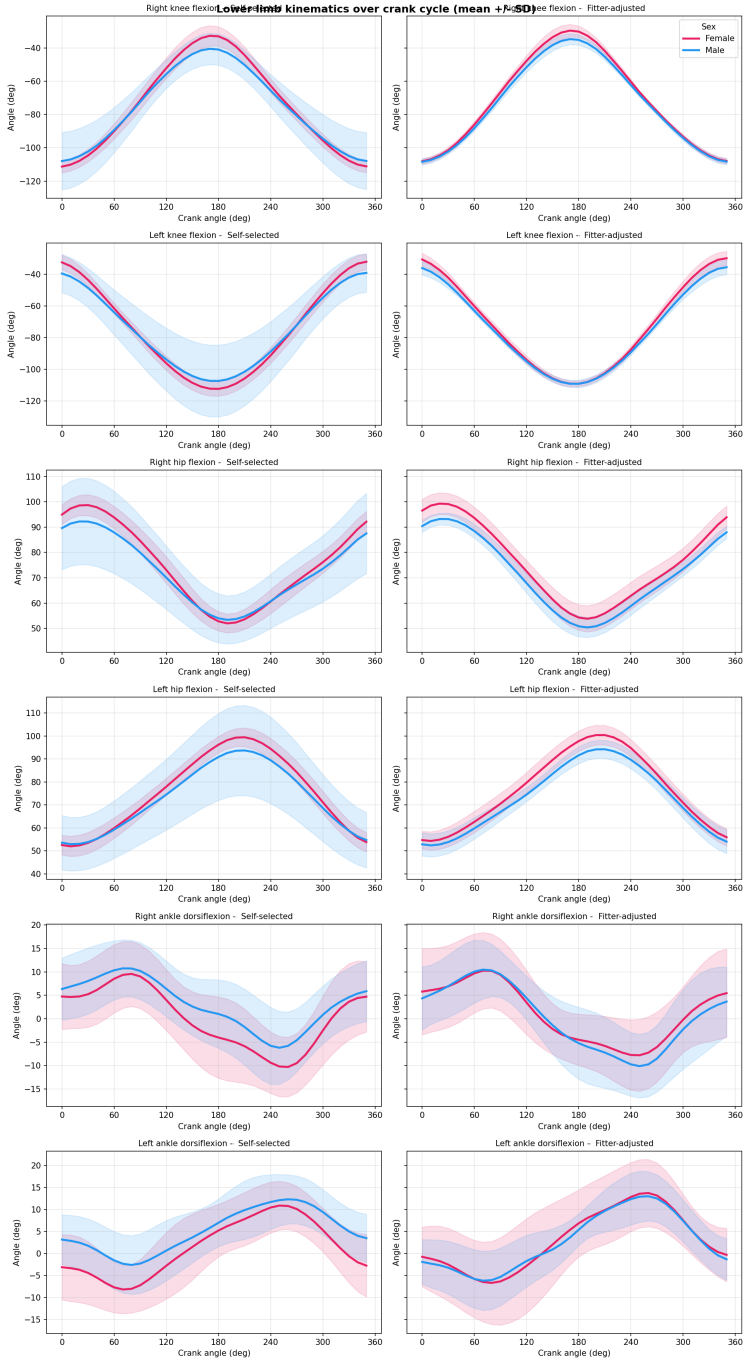


Fig. 17. Joint-angle trajectories (hip, knee, ankle flexion-extension; pelvic tilt) resolved over the normalised crank cycle (0-360°). Cohort mean ± SEM, S2 vs. S3 overlaid. Plots derived from the markerless Theia3D subset (n = 13 for S2, $n \sim 6$ for S3).

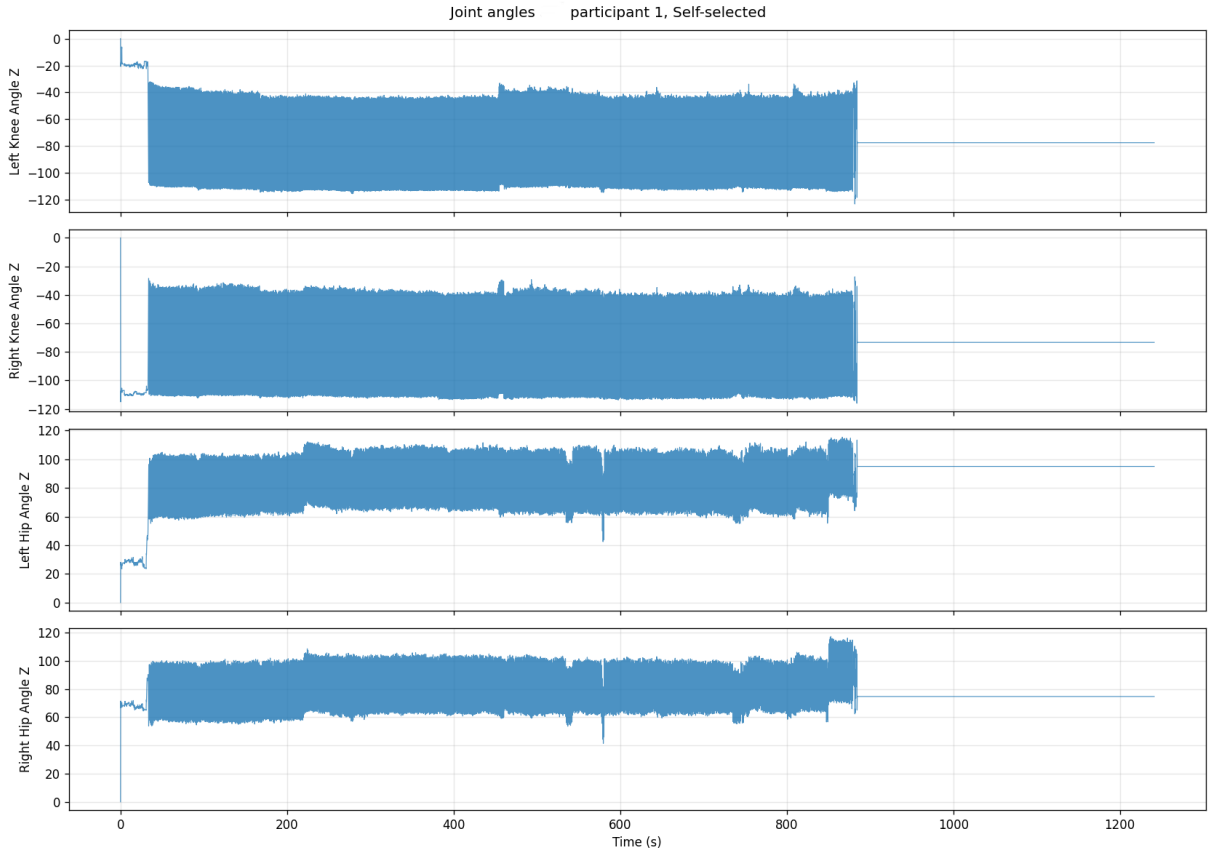


Fig. 18. Representative single-participant joint-angle traces (P01, S2) over the full 20-minute trial. Top: hip flexion. Middle: knee flexion. Bottom: ankle dorsiflexion.

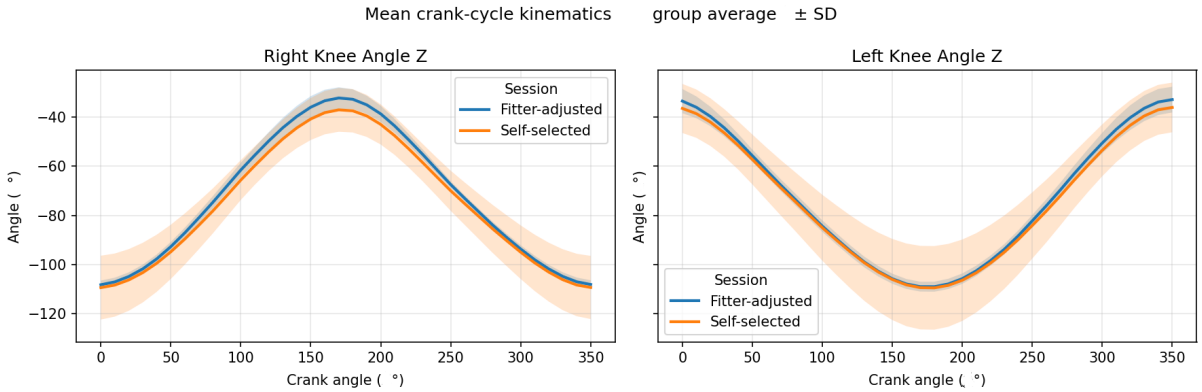
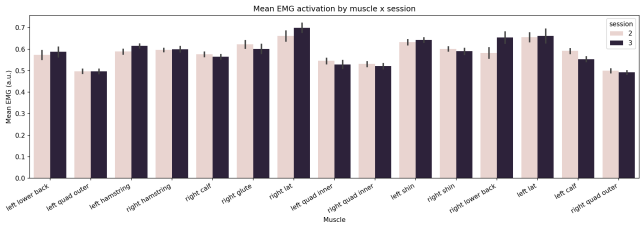


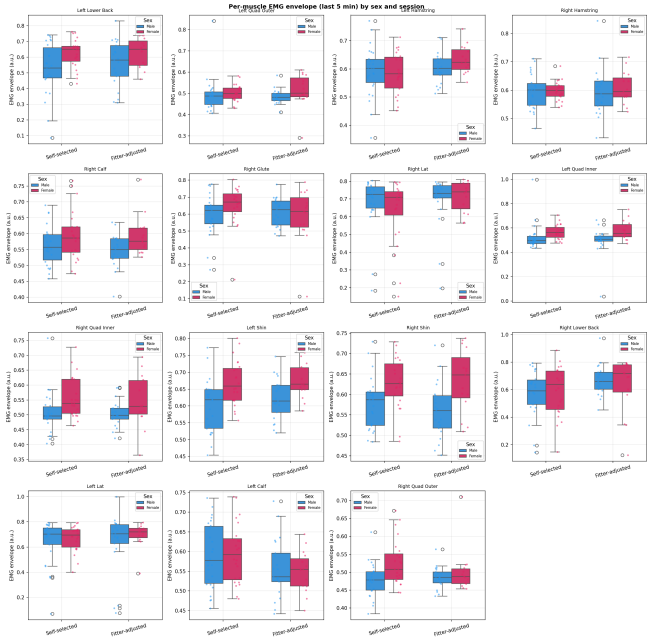
Fig. 19. Per-cycle joint-angle comparison between S2 and S3 for the motion-capture subset.

- Matthew Pearson

H.5 Neuromuscular Recruitment Patterns



(a) Mean EMG envelope by muscle and session (cohort).



(b) Per-muscle S2/S3 distributions split by sex.

Fig. 20. Global and per-muscle sEMG envelope (last 5 min mean, normalised to session peak).



Fig. 21. Sex×session EMG envelope heatmap across all 15 muscle sites. Values are last-5-minute mean, normalised. Rows = muscle, columns = Female/S2, Female/S3, Male/S2, Male/S3.

- Matthew Pearson

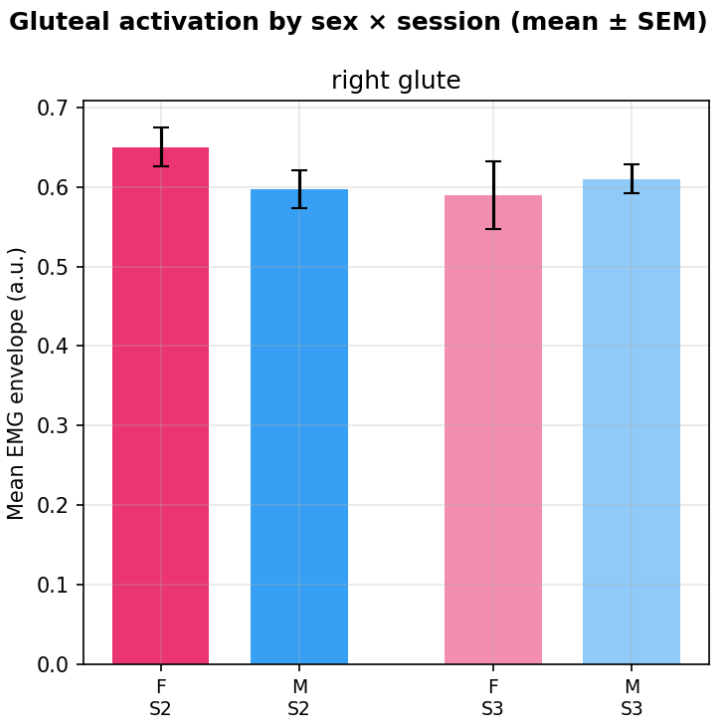


Fig. 22. Gluteus maximus sEMG envelope pre-/post-fit by sex, with per-participant paired change vectors. No significant sex×session interaction ($\eta_p^2 = 0.027$, $p = 0.34$).

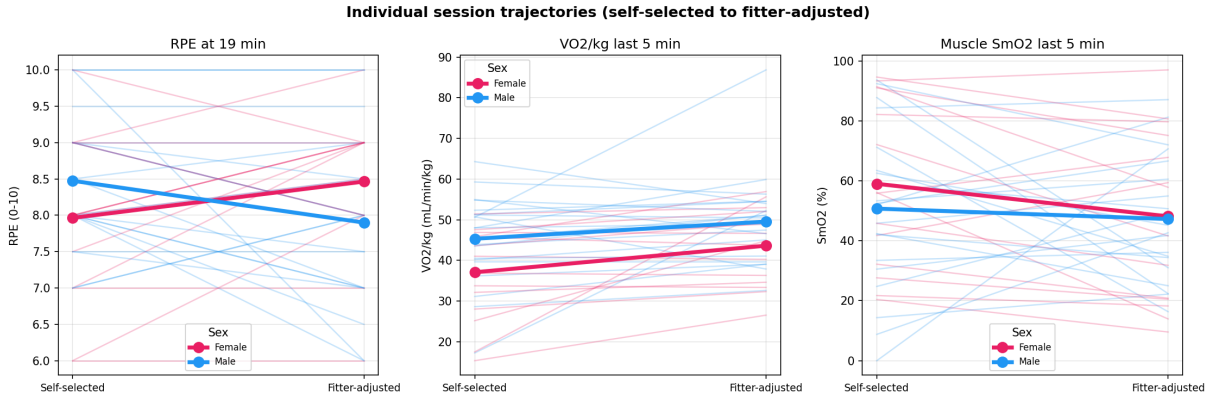


Fig. 23. Per-participant paired trajectories for the four largest-effect EMG variables; each line connects a single participant's S2 and S3 values.

Table 12. Co-contraction indices (CCI) for the two antagonist pairs defined in SectionSection 4.2. Reported from a two-way mixed ANOVA. No pair showed a sex×session interaction.

Pair	Source	F	p	η_p^2	Effect
Quad / Hamstring	Sex	0.45	0.509	0.013	negligible
Quad / Hamstring	Session	0.01	0.936	<0.001	negligible
Quad / Hamstring	Interaction	1.08	0.305	0.031	small
Tib. Ant. / Gastroc.	Sex	3.02	0.091	0.082	medium
Tib. Ant. / Gastroc.	Session	0.31	0.581	0.009	small
Tib. Ant. / Gastroc.	Interaction	0.30	0.587	0.009	small

- Matthew Pearson

H.6 Primary Hypothesis (H1): Full Paired-Effects Table

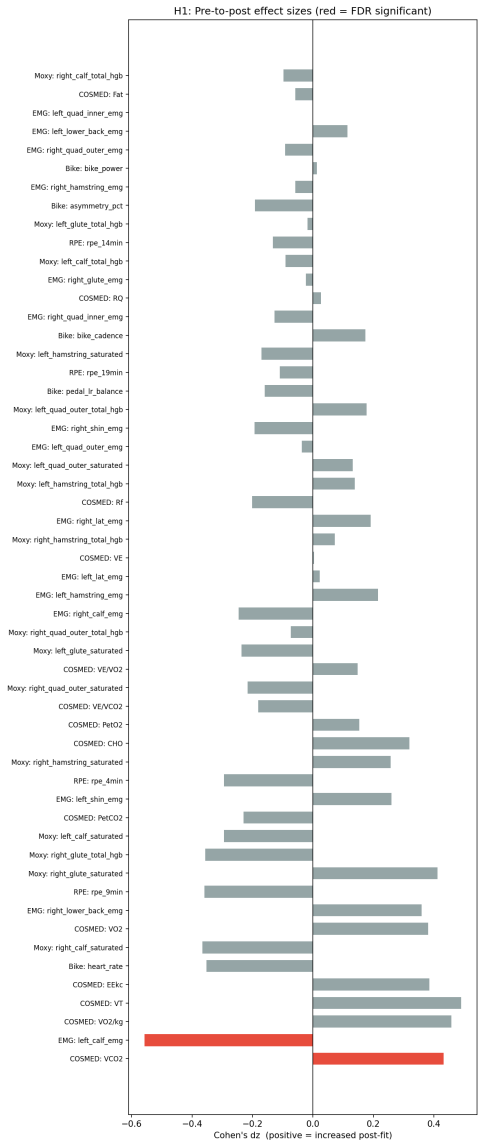


Fig. 24. Consolidated paired effect sizes (Cohen's d_z, S3−S2) grouped by sensor modality. Red markers are Benjamini-Hochberg FDR survivors at $q < 0.05$.

- Matthew Pearson



Fig. 25. Distribution of per-participant Δ-scores (S3−S2) for the top features surviving uncorrected $p < 0.05$.

Table 13. Full H1 paired-effects table (all 55 features from the unified matrix, $n = 36$). Sorted by uncorrected p. d_z = Cohen's d for paired data; W = Wilcoxon signed-rank statistic; p_{FDR} = Benjamini-Hochberg at $q < 0.05$. Source: `h1_prepost_overall.csv`.

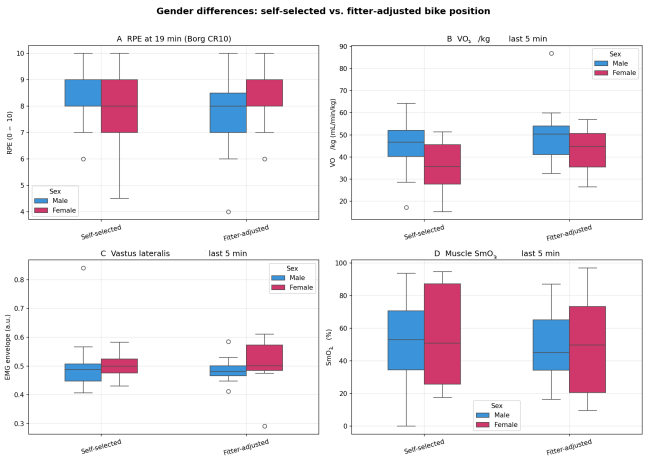
Modality	Variable	n	M_{S2}	M_{S3}	Δ	d_z	p	p_{FDR}	sig
COSMED	VCO_2 (ml min^{-1})	36	3018.7	3182.6	+163.8	+0.43	0.001	**0.024**	*
EMG	Left calf	36	0.595	0.553	−0.042	−0.56	0.001	**0.024**	*
COSMED	VO_2 kg^{-1}	36	41.88	47.06	+5.18	+0.46	0.003	0.053	
COSMED	V_T (L)	36	2.10	2.22	+0.12	+0.49	0.005	0.053	
COSMED	EE (kcal)	36	21466	23987	+2521	+0.39	0.005	0.053	
Bike	Heart rate (bpm)	36	173.2	162.0	−11.2	−0.35	0.010	0.086	
Moxy	Right calf SmO_2 (%)	35	43.66	36.24	−7.42	−0.37	0.013	0.100	
COSMED	VO_2 (ml min^{-1})	36	3204.9	3373.5	+168.6	+0.38	0.016	0.108	
EMG	Right lower back	36	0.586	0.654	+0.068	+0.36	0.041	0.221	
RPE	at 9 min	36	7.42	6.92	−0.50	−0.36	0.041	0.221	
Moxy	Right glute SmO_2 (%)	36	45.62	54.17	+8.55	+0.41	0.050	0.244	
Moxy	Right glute tHgb	36	21.41	19.50	−1.91	−0.36	0.060	0.270	
Moxy	Left calf SmO_2 (%)	35	43.73	38.73	−5.00	−0.29	0.065	0.270	
COSMED	$P_{et}CO_2$	36	74.33	36.52	−37.81	−0.23	0.074	0.287	
EMG	Left shin	36	0.622	0.643	+0.021	+0.26	0.095	0.332	
RPE	at 4 min	36	6.17	5.79	−0.38	−0.30	0.100	0.332	
Moxy	Right hamstring SmO_2	36	41.92	47.57	+5.65	+0.26	0.105	0.332	
COSMED	CHO ox. rate	34	2.89	3.12	+0.23	+0.32	0.134	0.375	
COSMED	$P_{et}O_2$	36	107.0	109.7	+2.70	+0.15	0.135	0.375	
COSMED	VE/VCO_2	36	35.97	32.41	−3.55	−0.18	0.139	0.375	
Moxy	R. quad outer SmO_2	34	33.75	30.43	−3.32	−0.22	0.168	0.420	
COSMED	VE/VO_2	36	30.89	41.32	+10.43	+0.15	0.176	0.420	
Moxy	Left glute SmO_2	34	54.13	47.62	−6.51	−0.24	0.179	0.420	
Moxy	R. quad outer tHgb	34	19.92	19.77	−0.16	−0.07	0.209	0.470	
EMG	Right calf	36	0.585	0.565	−0.020	−0.25	0.239	0.516	
EMG	Left hamstring	36	0.595	0.615	+0.020	+0.22	0.293	0.586	
EMG	Left lat	36	0.656	0.661	+0.005	+0.02	0.293	0.586	
COSMED	VE	36	97.92	97.97	+0.04	+0.00	0.371	0.715	
Moxy	R. hamstring tHgb	36	20.12	20.37	+0.24	+0.07	0.396	0.738	
EMG	Right lat	36	0.658	0.699	+0.041	+0.19	0.414	0.745	
COSMED	Rf (breaths min^{-1})	36	47.06	45.47	−1.59	−0.20	0.451	0.770	
Moxy	L. hamstring tHgb	35	19.74	20.27	+0.53	+0.14	0.461	0.770	
Moxy	L. quad outer SmO_2	35	29.97	31.86	+1.89	+0.13	0.471	0.770	
EMG	Left quad outer	36	0.500	0.497	−0.003	−0.04	0.539	0.857	
EMG	Right shin	36	0.604	0.590	−0.014	−0.19	0.581	0.897	
Moxy	L. quad outer tHgb	35	18.23	19.18	+0.95	+0.18	0.599	0.897	
Bike	Pedal L/R balance	15	50.04	49.30	−0.75	−0.16	0.639	0.897	
RPE	at 19 min	34	8.26	8.13	−0.13	−0.11	0.642	0.897	
Moxy	L. hamstring SmO_2	35	52.10	48.92	−3.18	−0.17	0.656	0.897	
Bike	Cadence (rpm)	36	86.50	88.03	+1.53	+0.17	0.669	0.897	
EMG	Right quad inner	36	0.533	0.522	−0.011	−0.13	0.681	0.897	
COSMED	RQ	36	0.943	0.945	+0.002	+0.03	0.762	0.923	
EMG	Right glute	36	0.605	0.601	−0.004	−0.02	0.786	0.923	
Moxy	Left calf tHgb	35	19.98	19.73	−0.24	−0.09	0.802	0.923	
RPE	at 14 min	36	7.79	7.58	−0.21	−0.13	0.835	0.923	
Moxy	Left glute tHgb	34	20.49	20.39	−0.10	−0.02	0.840	0.923	
Bike	Asymmetry %	15	6.97	6.00	−0.98	−0.19	0.847	0.923	
EMG	Right hamstring	36	0.604	0.599	−0.004	−0.06	0.858	0.923	
Bike	Power (W)	36	230.9	231.1	+0.15	+0.01	0.858	0.923	
EMG	Right quad outer	36	0.496	0.492	−0.004	−0.09	0.871	0.923	
EMG	Left lower back	36	0.569	0.587	+0.018	+0.11	0.895	0.923	
EMG	Left quad inner	36	0.529	0.529	+0.00	+0.00	0.895	0.923	
COSMED	Fat ox. rate	34	0.39	0.37	−0.02	−0.06	0.906	0.923	
Moxy	Right calf tHgb	35	20.53	20.18	−0.34	−0.10	0.929	0.929	

- Matthew Pearson

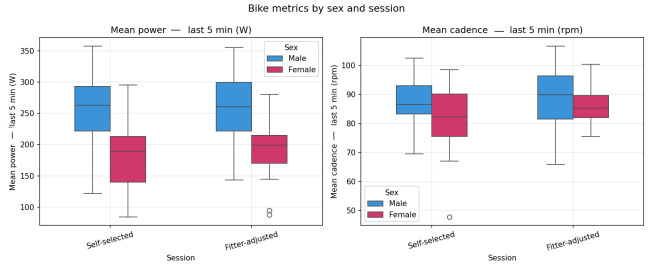
H.7 Sex-Stratified Statistics (H2)

Table 14. Full two-way mixed ANOVA (session × sex) results for every dependent variable tested. Source: `mixed_anova_results.csv`. Bold rows indicate the interaction term reached $p < 0.05$.

Variable	Source	F	p	η_p^2	Magnitude
VO_2/kg	Sex	5.27	0.028	0.134	medium
VO_2/kg	Session	7.40	0.010	0.179	medium
VO_2/kg	Interaction	0.36	0.553	0.010	negligible
VE	Sex	11.87	0.002	0.259	large
VE	Session	0.00	0.988	<0.001	negligible
VE	Interaction	3.17	0.084	0.085	medium
RQ	Sex	0.70	0.407	0.020	small
RQ	Session	0.03	0.875	0.001	negligible
RQ	Interaction	1.35	0.254	0.038	small
RPE 19 min	**Interaction**	**7.78**	**0.009**	**0.196**	**large**
L. lower back EMG	Sex	4.84	0.035	0.125	medium
L. lower back EMG	Interaction	0.38	0.540	0.011	negligible
L. quad outer EMG	Interaction	1.41	0.244	0.040	small
L. hamstring EMG	Interaction	3.21	0.082	0.086	medium
R. hamstring EMG	Interaction	0.27	0.607	0.008	negligible
R. calf EMG	Sex	4.45	0.042	0.116	medium
R. calf EMG	Interaction	1.32	0.259	0.037	small
R. glute EMG	Interaction	0.95	0.336	0.027	small

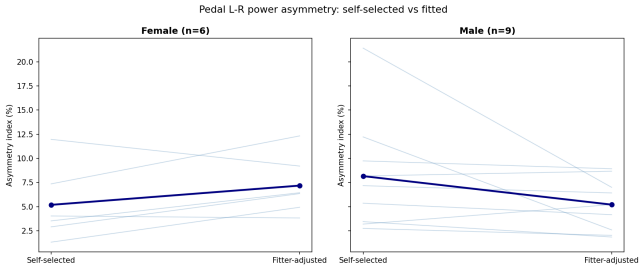


(a) Composite summary: demographics + key per-sex deltas.

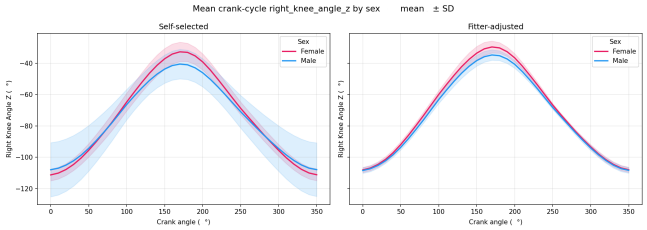


(b) Bike metrics (power, cadence, HR, asymmetry) by sex.

Fig. 26. Sex-stratified overview.



(a) Pedal left/right balance asymmetry Δ (S3−S2).

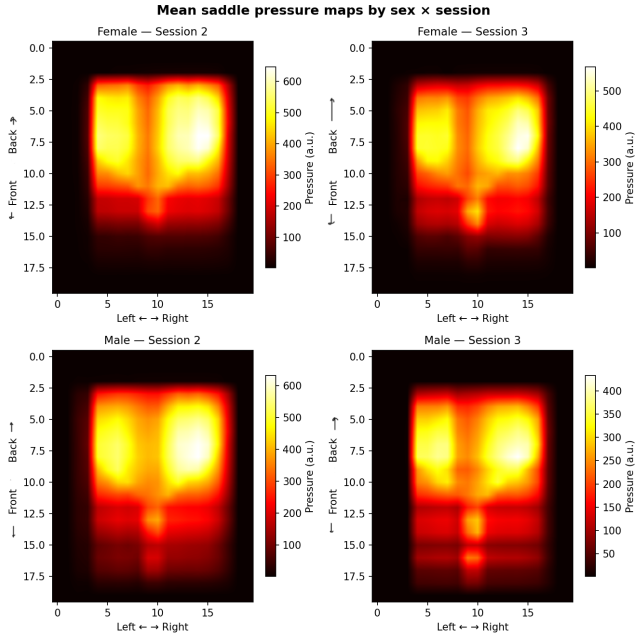


(b) Knee flexion Δ from available motion-capture subset.

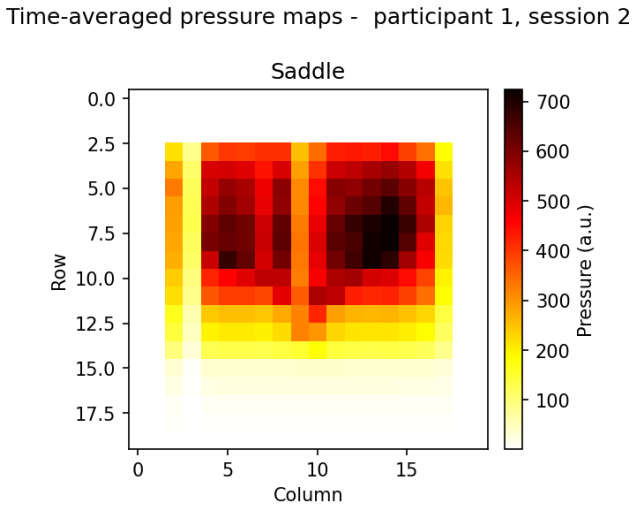
Fig. 27. Sex-specific responses for pedal balance ($p = 0.036$ on Δ, Mann-Whitney) and knee kinematics (descriptive, n limited).

Fig. 28. Effect of correction regime (raw p, Benjamini-Hochberg FDR, Bonferroni) on the count of surviving features at $\alpha = 0.05$. Used to separate stable from exploratory effects.

H.8 Saddle and Insole Pressure



(a) Cohort-average saddle pressure maps (20 × 20 cells).



(b) Example single-participant saddle pressure map (P01, S2).

Fig. 29. Saddle pressure distributions. Posterior COP shift is visible in the cohort-level map ($\Delta\text{COP}_y = +0.45$ cm, $d_z = +0.85$).

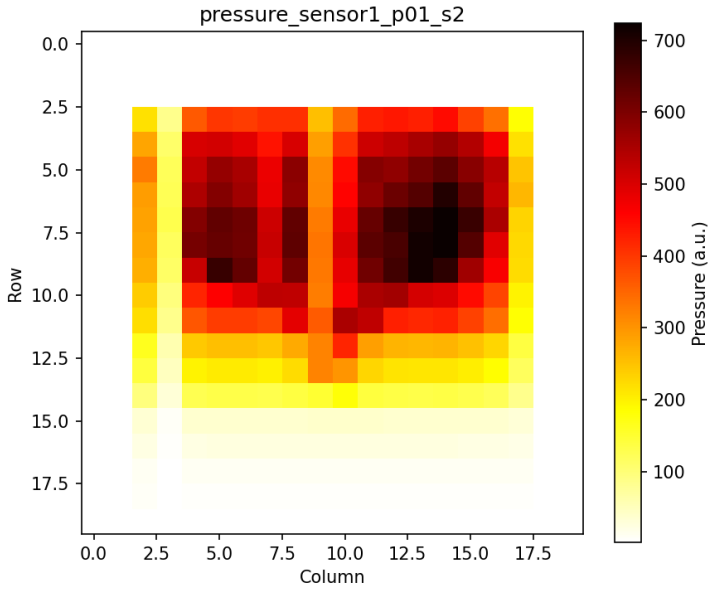


Fig. 30. Single-sensor mean insole pressure map (sensor 1, P01, S2) used to validate the custom pressure-mapping pipeline.

- Matthew Pearson

H.9 Multimodal Registration and Coupling (H4)

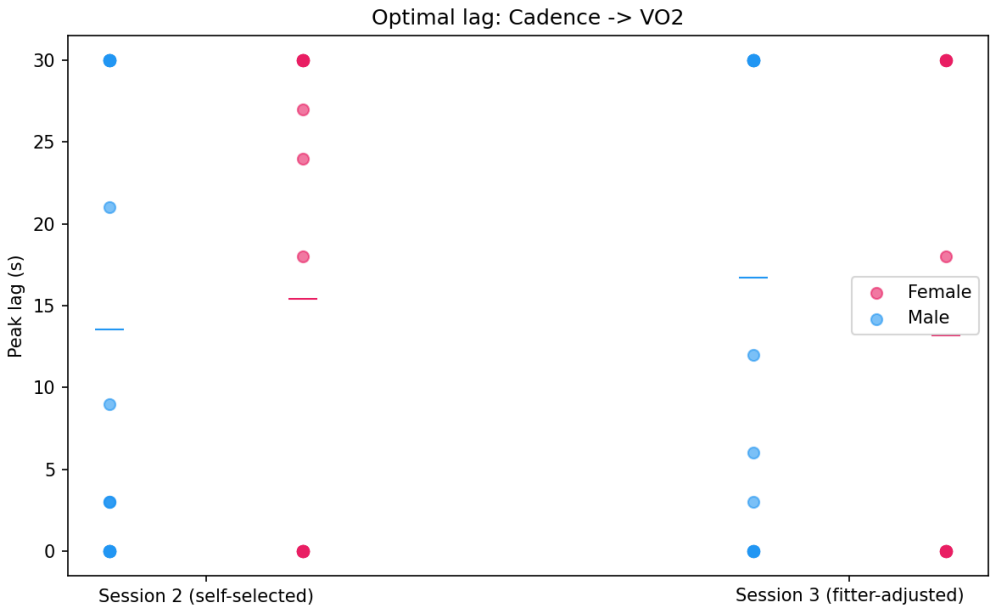


Fig. 31. Distribution of peak cadence→heart-rate cross-correlation lags across all 85 analysable trials. Median lag = 18 s, supporting the 12-16 s mechanical-to-metabolic lag literature (Procházka et al., 2017). Distribution does not differ by sex (χ^2 on $\{0, 1\text{-}29, 30\}$ s bins, $p = 0.42$).

Table 15. Cross-correlation lag distribution ($n = 85$ sessions).

Lag bin	Count	%
0 s (no lag detected)	35	41.2
1-29 s (within search window)	11	12.9
30 s (saturated at upper bound)	39	45.9
Median peak lag	18 s	

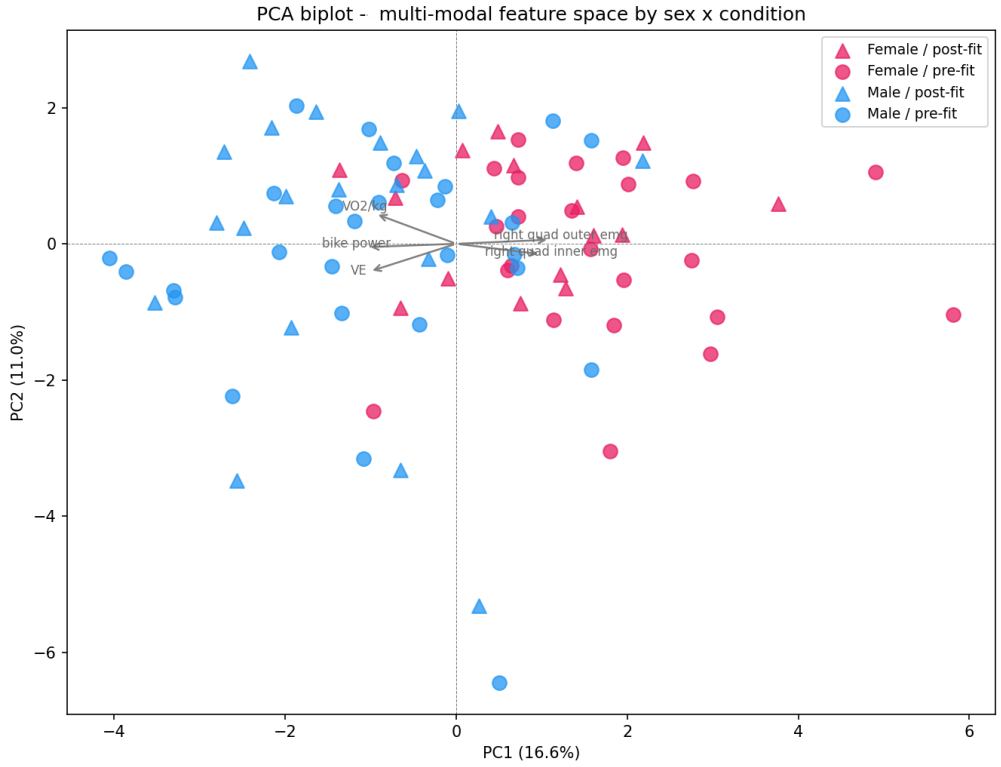


Fig. 32. PCA biplot of the unified feature matrix. PC1 captures 16.6% of variance, PC2 11.1%. Participants are marked by sex (colour) and session (shape). No clean S2-vs-S3 separation emerges on PC1-2; the fit signal is distributed across multiple neuromuscular features rather than a single principal axis.

Table 16. All cross-modal Spearman correlations with $|r_s| \geq 0.35$ on paired Δ-scores ($n = 36$, 253 pairs tested). Source: `crossmodal_spearman.csv`.

Variable 1	Variable 2	r_s	p
L. lower back EMG	R. lower back EMG	+0.64	<.001
R. lat EMG	L. lat EMG	+0.61	<.001
R. calf EMG	R. quad inner EMG	+0.54	0.001
RQ	R. lat EMG	−0.52	0.001
R. calf EMG	L. shin EMG	+0.48	0.003
VO_2/kg	L. hamstring EMG	+0.47	0.003
R. glute EMG	R. lower back EMG	+0.47	0.004
RQ	VO_2/kg	−0.45	0.006
VE	VO_2/kg	+0.44	0.007
R. lat EMG	R. lower back EMG	+0.43	0.009
L. lower back EMG	L. lat EMG	+0.42	0.011
VO_2/kg	R. lat EMG	+0.41	0.013
L. lower back EMG	R. lat EMG	+0.41	0.013
R. lower back EMG	L. lat EMG	+0.41	0.014
R. quad inner EMG	R. quad outer EMG	+0.39	0.018
R. glute EMG	L. lat EMG	+0.38	0.021
R. calf EMG	R. quad outer EMG	+0.38	0.023
VE	RPE at 19 min	+0.36	0.038
R. shin EMG	L. lat EMG	−0.35	0.039
L. hamstring EMG	L. lat EMG	+0.34	0.040

- Matthew Pearson

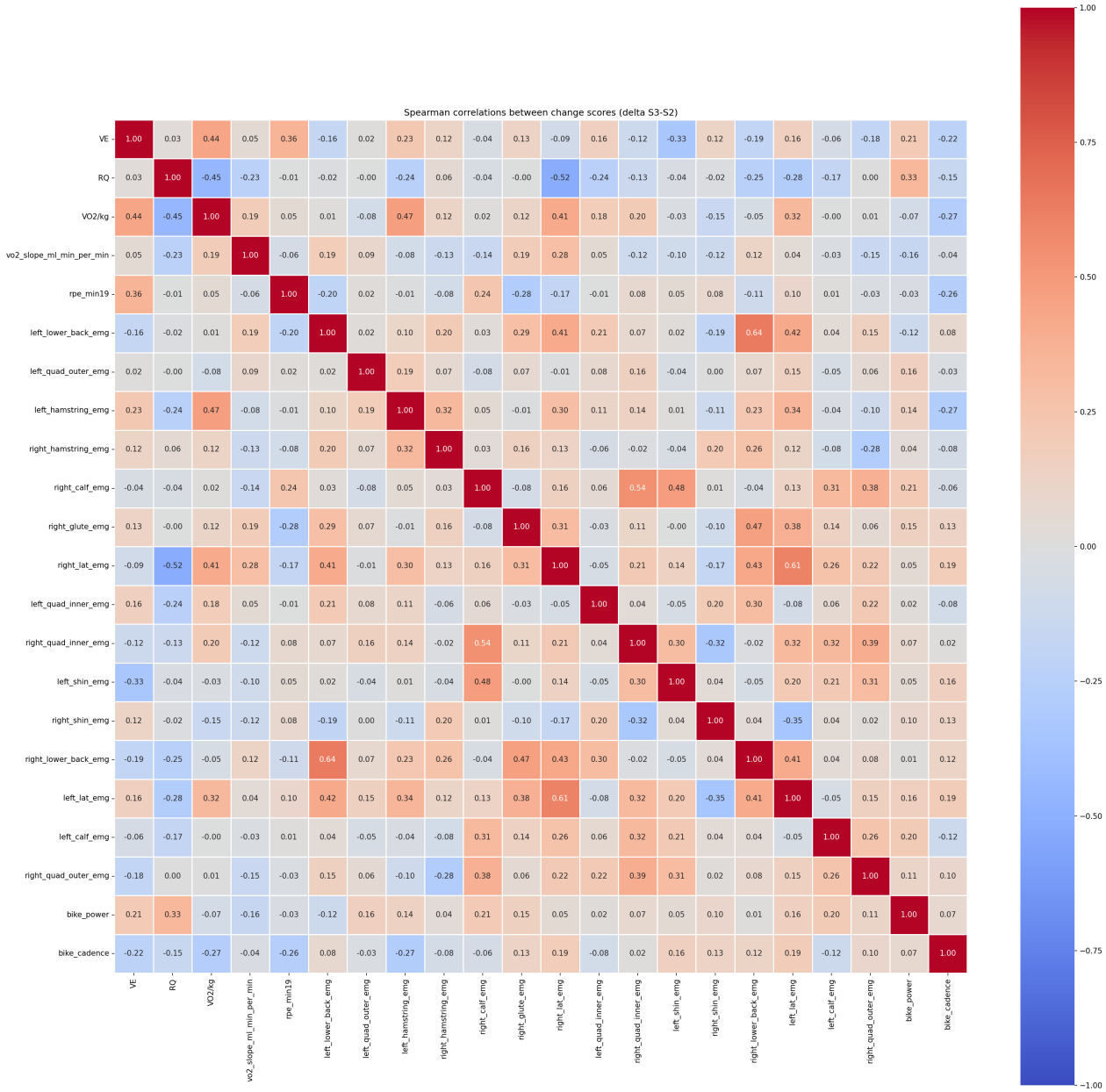


Fig. 33. Spearman correlation heatmap between paired Δ-scores (S3−S2) across all variables in the unified matrix. Strong within-EMG block (bilateral symmetry) is visible; cross-modal VO_2/kg↔hamstring and RQ↔lat couplings are the highlighted off-diagonal bands.

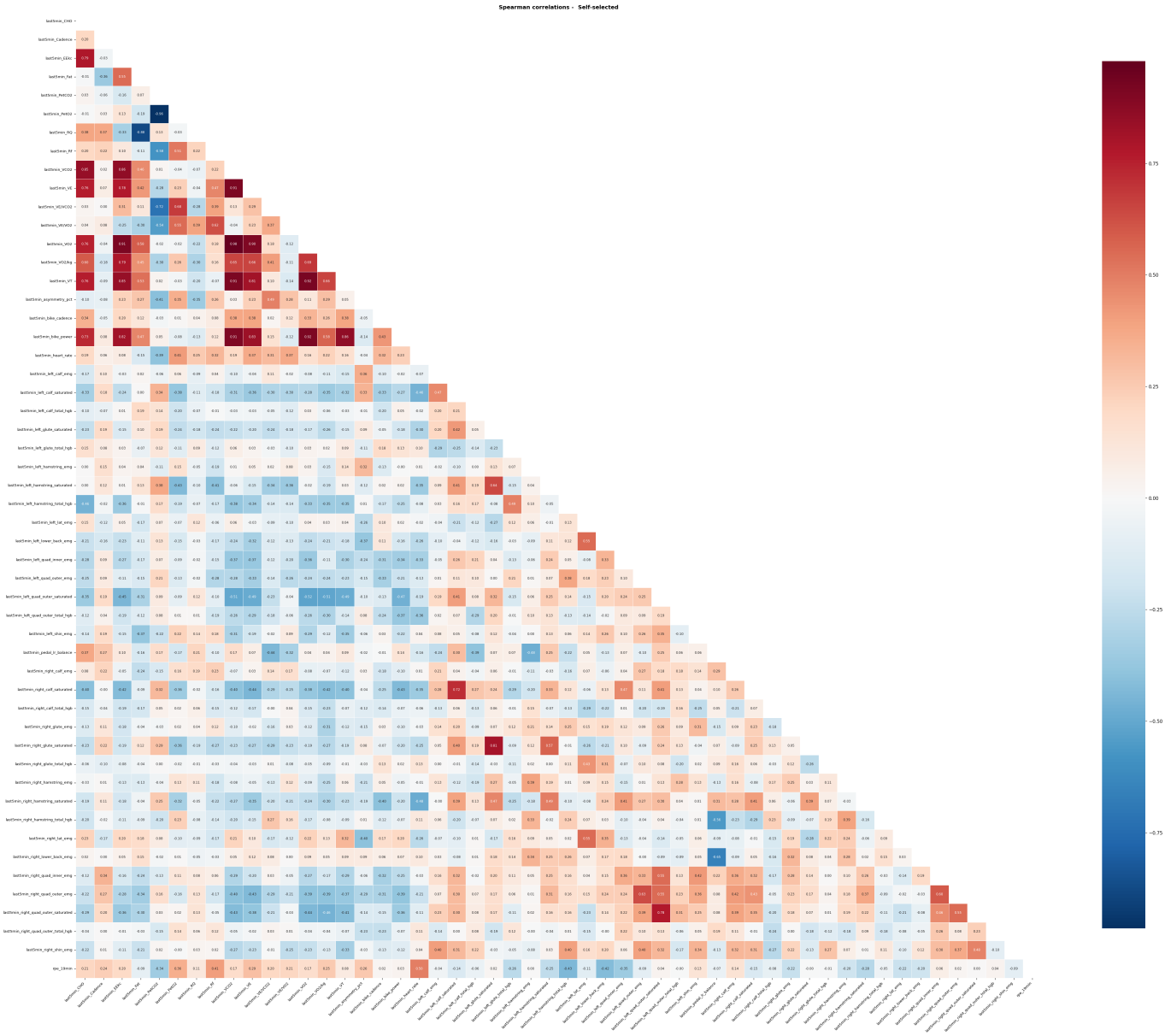


Fig. 34. Self-fitted (S2) correlation matrix across the full unified feature set.

- Matthew Pearson

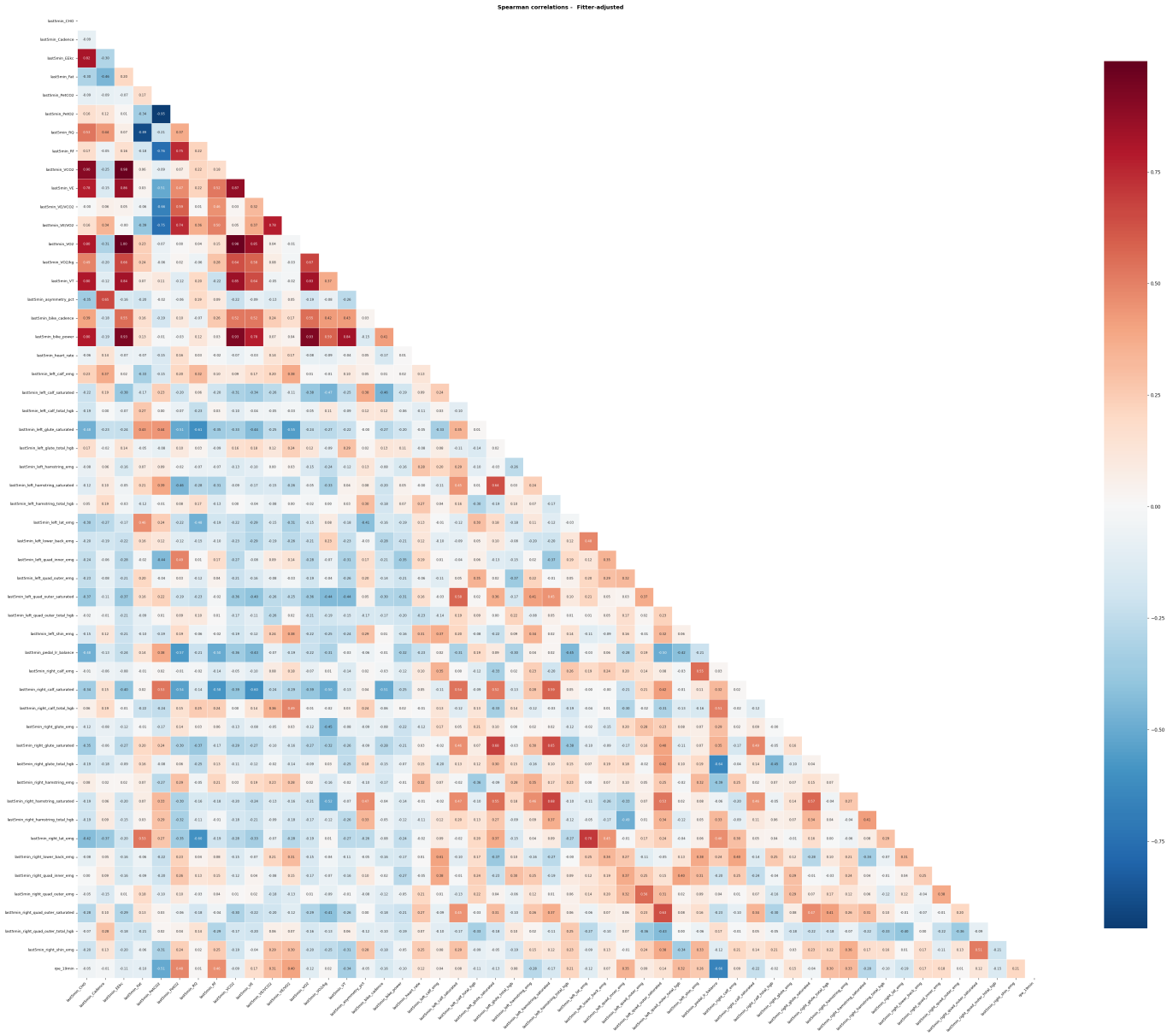


Fig. 35. Fitter-adjusted (S3) correlation matrix across the full unified feature set. Broadly comparable block structure supports the conclusion that cross-modal coupling does not differ categorically by fit condition.

H.10 Random-Forest Feature Importance (H3)

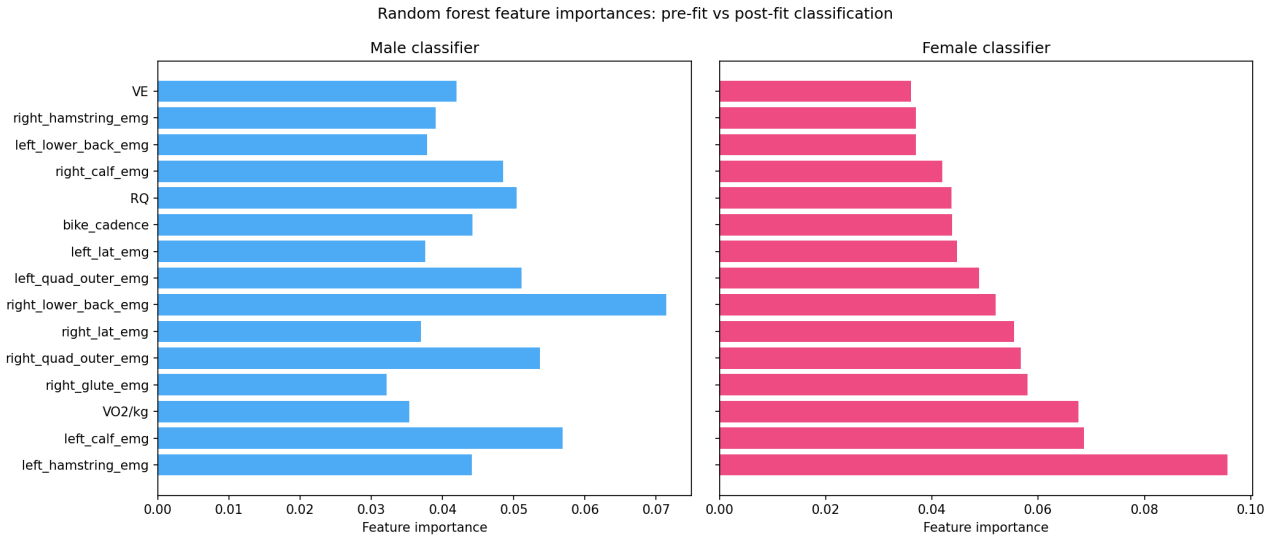


Fig. 36. Per-feature importance (mean decrease in Gini impurity) for the sex-stratified S2-vs-S3 random-forest classifiers. Features with the largest female−male gap (left hamstring EMG, right glute EMG, VO_2/kg) are highlighted.

Table 17. Full random-forest feature importance, sex-stratified classifiers (n = 15F / n = 21M). Sorted by female importance. Source: `rf_feature_importances.csv`.

Feature	Importance (F)	Importance (M)	F−M
Left hamstring EMG	0.0956	0.0441	+0.052
Left calf EMG	0.0686	0.0569	+0.012
VO_2/kg	0.0675	0.0353	+0.032
Right glute EMG	0.0580	0.0321	+0.026
Right quad outer EMG	0.0568	0.0537	+0.003
Right lat EMG	0.0555	0.0369	+0.019
Right lower back EMG	0.0520	0.0714	−0.019
Left quad outer EMG	0.0488	0.0511	−0.002
Left lat EMG	0.0448	0.0375	+0.007
Bike cadence	0.0438	0.0442	−0.0004
RQ	0.0436	0.0504	−0.007
Right calf EMG	0.0420	0.0485	−0.007
Left lower back EMG	0.0370	0.0378	−0.001
Right hamstring EMG	0.0370	0.0390	−0.002
VE	0.0360	0.0419	−0.006
RPE at 19 min	0.0359	0.0409	−0.005
Right quad inner EMG	0.0344	0.0363	−0.002
VO_2 slope	0.0310	0.0639	−0.033
Left quad inner EMG	0.0304	0.0421	−0.012
Right shin EMG	0.0289	0.0446	−0.016
Bike power	0.0286	0.0308	−0.002
Left shin EMG	0.0238	0.0605	−0.037

PARTICIPANT INFORMATION SHEET

Researchers
Hugo Hafner
hh2053@bath.ac.uk

Matthew Pearson
mp2457@bath.ac.uk

Supervisor
Eamonn O'Neill
maseon@bath.ac.uk

1. **What is the purpose of the project?**

The purpose of this project is to investigate bike fitting across different riders of different experience and of different sex to explore the driving components that make up a successful bike fit and how those may vary between any of the aforementioned groups.

2. **Do I have to take part?**

You do not have to take part in this project, and it is completely up to you if you would like to do so. Please ensure you carefully read this participant information sheet and follow up on any questions with the researchers before making a decision. Should you agree to take part, you will be asked to sign a consent form, however, if at any point during the process you no longer wish to participate, you will be able to withdraw without needing to provide any reasoning.

3. **What would taking part involve?**

Taking part would involve participation in 3 Lab Sessions, a summary of each and the expected durations are outlined below.

Lab session 1 (c. 60 mins):
Physical measurements are recorded: height, inside leg length, arm length, torso length, foot size, and body weight.
We will adjust the Wahoo Kickr bike using fitting equations e.g. Lemond based on your body measurements.
Resting heart rate will be assessed: lie quietly for 5 minutes, followed by 5 minutes of heart rate monitoring with a chest strap, this will be done in a private room.
You will then complete a Ramp test to estimate your Functional Threshold Power (FTP). This will determine the exercise intensity for subsequent sessions. This test consists of holding increasing levels of power for one-minute intervals. The Wahoo Kickr bike will be in erg mode and in a constant virtual gear.

Lab session 2 (c. 45 mins):
EMG, IMU and muscle oxygen sensors are attached to the following body locations: vastus lateralis (Outer head of the quad), gluteus maximus (glutes), Bicep Femoris (hamstring), and medial gastrocnemius (upper calf)
And extra EMG/IMU sensors will be applied to:
Latissimus dorsi (lats), Erector Spinae (lower back, singular)
Rectus Femoris (front head of quad), Tibialis Anterior (Front of the Shin), Deltoid (shoulder, singular)
You will be able to apply any sensors on your own if you choose, with a private room being available for this. We will aim to have at least one male and one female researcher per session, but please state if you have any preferences for this process for your own comfort. Please note that, as these sensors are attached to the skin, you may be asked to remove some hair if it is excessive. We will provide clean razors and shaving cream.

You will also be fitted with a heart rate monitor, a respiratory sensor and COSMED k5.
You will be asked to cycle at your FTP calculated from Lab Session 1 for 20 minutes.
You will report discomfort on a classic Borg scale (6-20) every 5 minutes.
Heart rate will be monitored following the exercise until it reaches below 100 bpm.

Lab session 3 (c. 2 hours):
Bike fitting session will be conducted on the Wahoo Kickr Bike.
New bike configuration measurements will be recorded.
You'll have a rest period and all sensors from the previous session will be applied again.
You will cycle at FTP calculated from Lab Session 1 for 20 minutes.
You will report discomfort on a classic borg scale (6-20) every 5 minutes.
Heart rate will be monitored following the exercise until it reaches below 100 bpm

4. **What are the exclusion criteria? (or are there reasons why I should not take part?)**

You should NOT take part if you currently have any musculoskeletal injuries or with cardiovascular contraindications for exercise.

5. **What are the possible benefits of taking part?**

Following the completion of all 3 Lab Sessions, you will be reimbursed £50 for your time. In the event of you withdrawing from the study early, you will be paid on a pro rata at the standard university rate of £12 an hour based on expected lab session durations.

6. **What are the possible risks of taking part?**

As with any physical activity, there is a risk of injury in taking part in our study. During the lab sessions, if at any point you feel uncomfortable, you are free to stop participating. You may then withdraw from the study completely or reschedule for a different day. Your decision to stop will be completely up to you, and you will not have to provide a reason, nor are there any consequences as a result.

7. **Who will have access to the information that I provide?**

All the information you provide will be treated as confidential, with only the research team (and the University governance staff where appropriate) having access to it.

8. **What will happen to the data collected and results of the project?**

All the information you provide will be treated as confidential and stored securely in a password protected file on the University of Bath's OneDrive, on a password protected device. The storage of the data will be in accordance with the UK's current data protection legislation. Recorded data will be stored securely and confidentially in the University's archives for a minimum of 10 years. No personal identifiable information will be disclosed in any presentation or publication of the research and any summary provided of the findings after the completion of the study will be generalised across all participants and will not contain any identifiable information. On completion of the project, other researchers at the University of Bath may conduct further research on the data that is collected; however, this will only occur on the fully anonymised data and on projects that are deemed favourable by the University of Bath ethics committee. Identifiable data (video recordings) will be deleted after our analysis is complete, the only remaining footage will be non-identifiable i.e. video of skeletal structure/joint angles in a 3D environment.

9. **How can I withdraw from the project?**

Should you wish to withdraw from this research at any point before completion of all Lab Sessions, you can let the researcher know in person or by email. If you wish to withdraw your data from the study following the completion of all Lab Sessions, please contact one of the researchers within 2 weeks of your participation. After this date it will not be possible to withdraw your data as some of the results may have been anonymised or analysed.

10. **University of Bath Privacy Notice**

The University of Bath privacy notice can be found here: https://www.bath.ac.uk/corporate-information/university-of-bath-privacy-notice-for-research-participants/.

11. **What happens if there is a problem?**

If you have any concerns regarding any aspect of the project, you should reach out to the researchers directly, who will do their best to answer any questions. If they are unable to resolve your concern or you wish to make a complaint regarding the project, please contact the Research Governance and Compliance Team at research-ethics@bath.ac.uk.

12. **Who should I contact if there is a problem?**

Please do not hesitate to contact any of the researchers or the project supervisor if you would like more information:

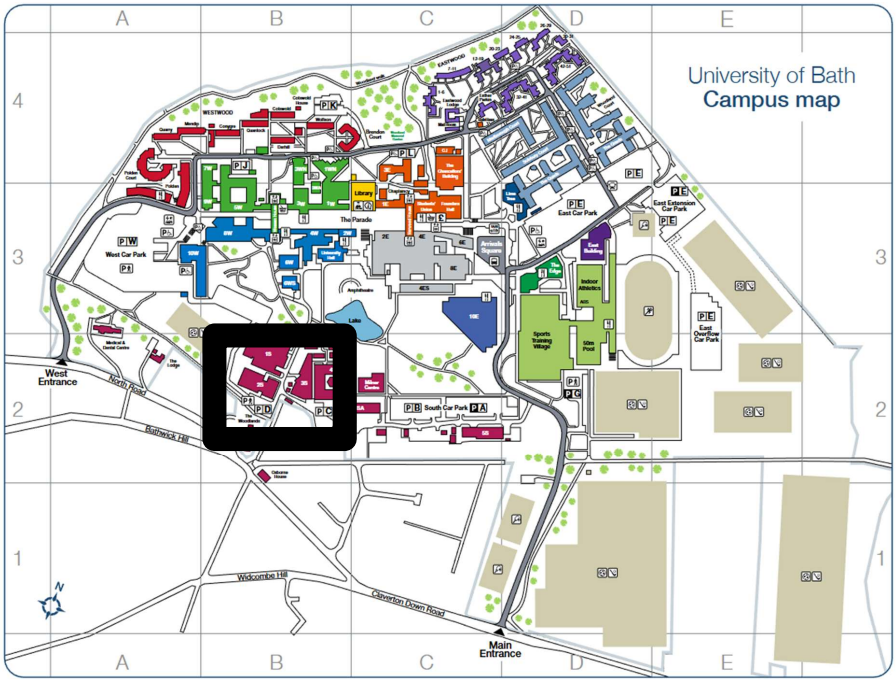
13. What should I bring to sessions?

Please bring clothes you are comfortable exercising in. For the purpose of the motion capture (in lab sessions 2/3) it would be ideal if these are not overly baggy clothes. If you have cleats/cycling shoes, please bring them. We have pedals that will fit SPD, SPD SL and Look cleats as well as flat pedals for those without cycling cleats. Bib straps can be used, but sensors will need to be placed on the upper body, so they should only be fully on after sensors are in place, to avoid continuous changing (sessions 2/3).

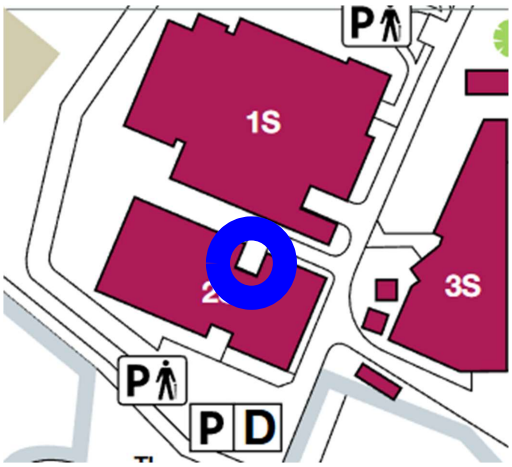
14. What to avoid before sessions?

We ask that you refrain from taking stimulants (e.g. caffeine, nicotine) and alcohol for the 24 hours before sessions. We also ask that you avoid vigorous exercise for the 24 hours before sessions.

All three lab sessions will take place in 2 South 0.35. The building is restricted to key card access, so please call one of the researchers when you arrive. A map of the university campus is below if needed



Please go towards the North entrance of the building



We will provide water for sessions if needed, but feel free to bring your own bottle. There are toilets in the building, but not showers.

Researchers
Hugo Hafner
hh2053@bath.ac.uk

Matthew Pearson
mp2457@bath.ac.uk

Supervisor
Eamonn O'Neill
maseon@bath.ac.uk

J Participant Consent Form

CONSENT FORM

The Impact of Professional Bike Fitting on Biomechanical and Physiological Efficiency.

Name of researcher: Matt Pearson, Hugo Hafner
Contact details of researcher: mp2457@bath.ac.uk, hh2053@bath.ac.uk

Name of Supervisor / Co-investigator: Eamonn O'Neill, Crescent Jicol
Contact details of Supervisor / Co-investigator: maseon@bath.ac.uk, cj406@bath.ac.uk

Please initial box if you agree with the statement

1. I have been provided with information explaining what participation in this project involves.
2. I have had an opportunity to ask questions and discuss this project.
3. I have received satisfactory answers to all questions I have asked.
4. I have received enough information about the project to make a decision about my participation. ☐
5. I understand that I am free to withdraw my consent to participate in the project at any time without having to give a reason for withdrawing.
6. I understand that I am free to withdraw my data within two weeks of my participation. ☐
7. I understand the nature and purpose of the procedures involved in this project. These have been communicated to me on the information sheet accompanying this form. ☐
8. I understand that the University of Bath may use the data collected for this study in future research project(s) but that the conditions on this form under which I have provided the data will still apply. ☐
9. I understand that I will have sensors placed and taped onto a number of muscle groups, including quads, calves, hamstrings, glutes (done in private by yourself), back and shoulders ☐
10. I understand that I will be recorded during sessions for the purpose of motion capture. ☐
11. I understand the data I provide will be treated as confidential, and that on completion of the project my name or other identifying information will not be disclosed in any presentation or publication of the research.
12. I agree to the University of Bath keeping and processing the data that I provide during the course of this study and my consent is conditional upon the University complying with its duties and obligations under the Data Protection Act. ☐

☐

13. I hereby fully and freely consent to my participation in this project. ☐

Participant's signature: _____ Date: _____

Participant name in BLOCK Letters: _____

Researcher's signature: _____ Date: _____

Researcher name in BLOCK Letters: _____

If you have any concerns or complaints related to your participation in this project please direct them to the researchers named above.

K Participant Debreif Sheet

PARTICIPANT DEBRIEF DOCUMENT

Dear [[Name]],
Thank you for taking part in our research project. The information you provided today will greatly aid our study and help us to gain a much better understanding of how best bike fitting science can advance in future.

All the information you provided will be treated as confidential and stored securely in a password protected file on the University of Bath's OneDrive, on a password protected device. The storage of the data will be in accordance with the UK's current data protection legislation. Recorded data will be stored securely and confidentially in the University's archives for a minimum of 10 years. No personal identifiable information will be disclosed in any presentation or publication of the research and any summary provided of the findings after the completion of the study will be generalised across all participants and will not contain any identifiable information. On completion of the project, other researchers at the University of Bath may conduct further research on the data that is collected; however, this will only occur on the fully anonymised data and on projects that are deemed favourable by the University of Bath ethics committee. Identifiable data (video recordings) will be deleted after our analysis is complete, the only remaining footage will be non-identifiable i.e. video of skeletal structure/joint angles in a 3D environment.

Should you wish to withdraw any information you have provided or that we have collected in our sessions, please reach out to any of us within the next 2 weeks. Following the 2 week period you will no longer be able to withdraw your data, as by this point it will have been anonymised and begun to be analysed.

Following the conclusion of our research project, should you wish to have any of our findings be shared with you, please reach out to any of the researchers.

On behalf of our team
Thank you again for your participation.

Researchers:
Hugo Hafner
hh2053@bath.ac.uk

Matthew Pearson
mp2457@bath.ac.uk

Supervisor
Eamonn O'Neill
maseon@bath.ac.uk

L Unstructured Interview with Tony Corke

Q: is there a demographic bias of people coming to get fitted?

A: 40-65yr old middle to upper income males 75%

Q: do you notice specific demos coming back and giving different feedback?

A. The who spend the most are usually the most enthusiastic. Otherwise not really.

Q. how do different fits alter feel of the bike? e.g. TT vs track vs casual road

A. I don't understand. Handling feel or body feel? E.g. what does it feel like to ride a TT bike?

Q. What type of fit were you conducting during the study?

A. Road gross positioning. No cleat adjustment unless needed. No saddle change or angle adjustment, no inner shoe adjustment, no bar width or hood adjustment

Q. Are you made aware of anatomical sex differences in fitting training?

A. somewhat, women can have longer legs, but not always, pelvis is generally different but not always, they tend to be more flexible and less strong but not always, they tend to have weaker arms and shoulders but not always. Of course they do have different genitalia. There is so much individual variation in both sexes that generalisations become pretty unhelpful when trying to optimise the individual

Q. Are there any difficulties in communication in the fitting process e.g. talking about pressure on genitals?

A. The difficulty in communicating is great. I am an expert in it so make it look easy. We are trying to get our cyclist to verbalise small sensations that they have mostly never experienced, let alone have words for. They are such small sensations that they go largely unnoticed in a real world bike ride. Not every one feels the same physiological stress in the same area of thier body or in the same way. One of the challenges is building language with the rider without falsely leading them to say what you want to hear I have no issues talking about genitalia, however some people or nationalities might

Q. What things are tested during standard bike fits that we did not have the time/hardware to test in the experiment?

A. So in our fitting we assessed cleat position (fore/aft) saddle height, saddle setback, reach to bars, bar height, weight distribution and crank length for range of movement Body weight distribution. Feel of mass through contact points with the goal of trying to minimise weight through the hands without sacrificing ease of pedaling or power production

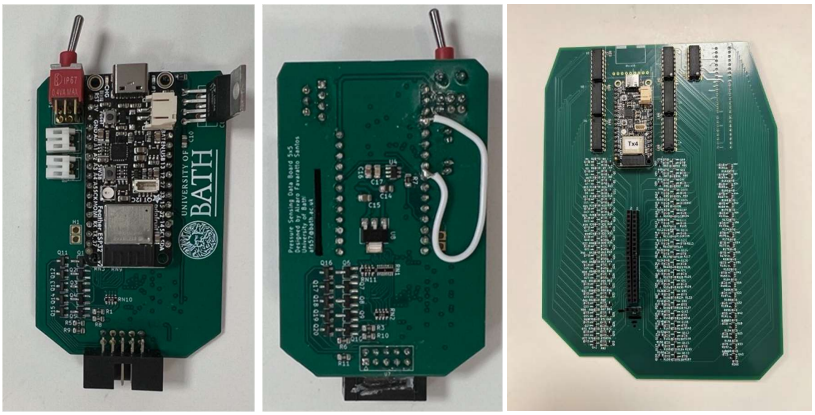
M Hardware Overview

- Matthew Pearson

N Hardware Information (Authored by Alvaro Favaratto Santos

Pressure sensing:

We needed a device that was able to map pressure from a surface, sending its data wirelessly from the Data Acquisition board into a server.



The prototype is divided into two distinct parts, one is the data acquisition board, that is responsible for:

- multiplexing (a process that sweeps through multiple sensing cells rapidly and with minor noise/disruption of the signal)
- Signal treatment via hardware (so we get a proportional signal, that goes up as the pressure on the pressure sensor goes up, instead of the untreated response, that exhibits the reverse).
- Isolate and deal with the values of the pressure sensor exclusively using clever circuitry rather than simplistic approaches with voltage dividers

The second distinct part is the pressure sensors, that are categorized mainly in two modes:

Thru mode (High Sensitivity), that is used in the saddle. This mode is constructed by using a meta material (that changes its resistance proportionally with pressure applied to it) in between two flexible PCBs with traces “sandwiching” the meta material. As pressure is applied, the meta material is compressed, and the current flow vertically from the top PCB to the bottom PCB.
This was used on the saddle sensor.



Shunt mode (High force range), where we only have two layers, one containing the meta-material, while the other contains copper traces designed in an inter-digit arrangement. This means that the current is travelling horizontally rather than vertically.

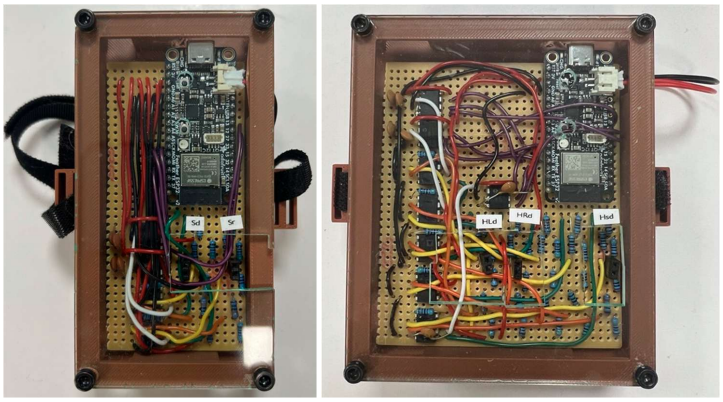
This was used on the insoles and handlebar.



Thru mode was the initial design of the pressure sensors, due to its simplicity in design and intuitive mechanics. As the project progressed, we realized that, while the saddle did work well for the project, the same was not true when dealing with the insoles. That was due mainly to the more complex geometry of the insole, that was particularly challenging when designing pressure cells that had the same properties (cell sizes, distances between cells), that left the insoles unreliable and too sensitive.

After evaluating the construction of Force Sensitive Resistors in the market, I realised the distinction between the two modes, and after manufacturing some test sheets (going through the different geometrical values), we found a suitable design for our pressure sensing board.

Strain gauge board:



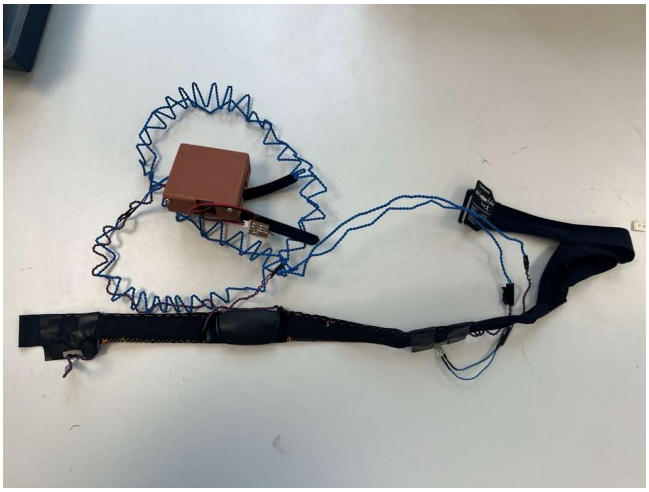
Strain gauge is a device that can measure deflections (contraction and expansion).

The changes are very small (3% over its baseline value of 350 Ohms), requiring considerable amplification.

We selected an amplification of 200X, placing the changes into a level that the microcontroller can interpret via its Analog to Digital Converter (ADC).

The circuit does have a variation between the seat post and the handlebar, and that is due to the number of inputs (handlebar have 3 strain gauges, one for its axis rotation, and the two remaining for the deflection on the left and right side of the handlebar, while the seat post pole measures its deflection and rotation).

Respirator Belt:



This sensor is a combination of:

1- A Garmin Heart rate sensor
2- A circuit that measures the pressure of the belt when compressed against the user's chest via Force Sensitive Resistors (FSR) in the left and right side of the belt. Those values are then sent wirelessly to the webpage.

The device is also able to broadcast the data via WIFI (also being able to broadcast Bluetooth).

Both data streams are broad casted separately.

O AI Acknowledgment

Claude Code (Opus 4.7, from Anthropic at https://claude.ai/) was used to validate which data correction techniques and statistics to use. It was also used to do a pass of the codebase to ensure there was no unused blocks or old comments. It was also used to clean up the two markdown files, with formatting suggestions to ensure that they would be readable. The same model was used for formatting suggestions in this report i.e. how to fit in larger graphs and tables without breaking the page layout. The same model was also used to run a grammar check on this report.

The ideas, structure and processing was my own work